

Cell Wall Remodeling Enzymes Modulate Fungal Cell Wall Elasticity and Osmotic Stress Resistance

Iuliana V. Ene,^{a*} Louise A. Walker,^{a*} Marion Schiavone,^{b,c,d} Keunsook K. Lee,^a H el ene Martin-Yken,^{b,c,d} Etienne Dague,^{e,f} Neil A. R. Gow,^a Carol A. Munro,^a Alistair J. P. Brown^a

School of Medical Sciences, University of Aberdeen, Institute of Medical Sciences, Foresterhill, Aberdeen, United Kingdom^a; Universit e de Toulouse; INSA, UPS, INP, LISBP, Toulouse, France^b; INRA, UMR792 Ing enierie des Syst emes Biologiques et des Proc ed es, Toulouse, France^c; CNRS, UMR5504, Toulouse, France^d; CNRS, LAAS, Toulouse, France^e; Universit e de Toulouse, LAAS, Toulouse, France^f

* Present address: Iuliana V. Ene, Department of Molecular Microbiology and Immunology, Brown University, Providence, Rhode Island, USA; Louise A. Walker, Department of Molecular and Biomedical Sciences, University of Maine, Orono, Maine, USA.

ABSTRACT The fungal cell wall confers cell morphology and protection against environmental insults. For fungal pathogens, the cell wall is a key immunological modulator and an ideal therapeutic target. Yeast cell walls possess an inner matrix of interlinked β -glucan and chitin that is thought to provide tensile strength and rigidity. Yeast cells remodel their walls over time in response to environmental change, a process controlled by evolutionarily conserved stress (Hog1) and cell integrity (Mkc1, Cek1) signaling pathways. These mitogen-activated protein kinase (MAPK) pathways modulate cell wall gene expression, leading to the construction of a new, modified cell wall. We show that the cell wall is not rigid but elastic, displaying rapid structural realignments that impact survival following osmotic shock. Lactate-grown *Candida albicans* cells are more resistant to hyperosmotic shock than glucose-grown cells. We show that this elevated resistance is not dependent on Hog1 or Mkc1 signaling and that most cell death occurs within 10 min of osmotic shock. Sudden decreases in cell volume drive rapid increases in cell wall thickness. The elevated stress resistance of lactate-grown cells correlates with reduced cell wall elasticity, reflected in slower changes in cell volume following hyperosmotic shock. The cell wall elasticity of lactate-grown cells is increased by a triple mutation that inactivates the Crh family of cell wall cross-linking enzymes, leading to increased sensitivity to hyperosmotic shock. Overexpressing Crh family members in glucose-grown cells reduces cell wall elasticity, providing partial protection against hyperosmotic shock. These changes correlate with structural realignment of the cell wall and with the ability of cells to withstand osmotic shock.

IMPORTANCE The *C. albicans* cell wall is the first line of defense against external insults, the site of immune recognition by the host, and an attractive target for antifungal therapy. Its tensile strength is conferred by a network of cell wall polysaccharides, which are remodeled in response to growth conditions and environmental stress. However, little is known about how cell wall elasticity is regulated and how it affects adaptation to stresses such as sudden changes in osmolarity. We show that elasticity is critical for survival under conditions of osmotic shock, before stress signaling pathways have time to induce gene expression and drive glycerol accumulation. Critical cell wall remodeling enzymes control cell wall flexibility, and its regulation is strongly dependent on host nutritional inputs. We also demonstrate an entirely new level of cell wall dynamism, where significant architectural changes and structural realignment occur within seconds of an osmotic shock.

Received 13 June 2015 Accepted 13 July 2015 Published 28 July 2015

Citation Ene IV, Walker LA, Schiavone M, Lee KK, Martin-Yken H, Dague E, Gow NAR, Munro CA, Brown AJP. 2015. Cell wall remodeling enzymes modulate fungal cell wall elasticity and osmotic stress resistance. *mBio* 6(4):e00986-15. doi:10.1128/mBio.00986-15.

Editor John W. Taylor, University of California

Copyright   2015 Ene et al. This is an open-access article distributed under the terms of the [Creative Commons Attribution-Noncommercial-ShareAlike 3.0 Unported license](https://creativecommons.org/licenses/by-nc-sa/4.0/), which permits unrestricted noncommercial use, distribution, and reproduction in any medium, provided the original author and source are credited.

Address correspondence to Alistair J. P. Brown, al.brown@abdn.ac.uk.

The cell wall is essential for the integrity of the fungal cell, providing strength and shape to the growing cell, as well as protection against environmental insults. The robustness of the cell wall is critical for the maintenance of fungal morphology in all fungi studied to date. Mutations that perturb the molecular integrity of the cell wall result in the loss of spatial form for ovoid, pseudohyphal, and hyphal cells and, often, lysis and death (1–3). For pathogenic fungi, the cell wall is also the initial point of contact with the host, and cell wall components modulate fungal interactions with immune defenses (4–7). Furthermore, many features of fungal cell wall biosynthesis are unique to fungi and are consequently viewed as excellent targets for antifungal drug

development (8–12). The cell walls of the major opportunistic fungal pathogen, *Candida albicans*, are mainly comprised of β -1,3- and β -1,6-glucans (glucose polymers), chitin (an *N*-acetylglucosamine polymer), and mannoproteins (8, 13–16). β -glucans account for about 50 to 60% of cell wall biomass, forming a three-dimensional matrix of locally aligned β -1,3-glucan molecules that encircle the cell, to which shorter β -1,6-glucan polymers are covalently attached (15, 17). Indeed, chitin and β -1,3- and β -1,6-glucans represent the common architectural signature of the cell walls of most fungal species that have been investigated to date.

Mannoproteins represent about 30 to 40% of *C. albicans* cell

wall biomass, generating the outer fibrillar layer of the cell wall. There are two main types of mannoproteins in the yeast cell wall, the majority being glycosylphosphatidylinositol (GPI)-modified proteins that are covalently linked to the β -glucan network via β -1,6-glucan. The other mannoproteins are “proteins with internal repeats” (Pir proteins), which are attached to β -1,3-glucan via alkali-sensitive bonds (10, 18). Cell wall proteins, which are generally heavily mannosylated via *O*- and *N*-linkages (19–22), include structural molecules, cell wall remodeling enzymes, adhesins, and invasins that promote pathogenicity as well as contributing to cell wall integrity (23, 24).

Chitin represents a relatively minor component of the cell wall in terms of biomass (1 to 3%) but is essential for cell viability in all fungal species where it has been investigated (25). Chitin polymers, which are covalently cross-linked to the β -glucan network, are thought to contribute to the rigidity and physical strength of the yeast cell wall (13–15, 26, 27). The cross-linking between cell wall macromolecules is catalyzed by carbohydrate active cell wall remodeling enzymes that are located in the cell wall (28, 29). These cell wall remodeling enzymes include the Gas-like family of β -1,3-glucanosyltransferases (Phr1, Phr2, Pga4, and Pga5; CAZy glycoside hydrolase family) (72) and the Crh family of chitin-glucanosyltransferases (Crh11, Crh12, and Utr2; CAZy glycoside hydrolase family 16) (3, 24, 30–33).

The yeast cell wall is generally viewed as a rigid structure that confers shape and robustness to the fungal cell when it is faced with environmental insults (8, 13–15, 27). Indeed, cell wall biosynthesis has been used as a basis for models of polarized growth (34, 35). However, F. Klis and others have highlighted the flexibility of the yeast cell wall in terms of new cell wall growth and cellular adaptation to environmental change (10, 12, 23, 36, 37). Significant changes in the *C. albicans* cell wall proteome are observed following growth in different morphologies, at different ambient pHs and temperatures, and on different nutrients (38–41). Also, following exposure to antifungal drugs, *C. albicans* triggers cell wall remodeling mechanisms that influence the expression of chitin, β -glucan, and mannan biosynthetic genes and that lead to alterations in the cell wall proteome (37, 41–44). Environmental inputs therefore induce changes in the content and architecture of the new cell wall as it is synthesized, many of these changes being manifested by alterations in gene expression.

In this report, we reveal a new level of dynamism of the yeast cell wall that involves dramatic changes in cell wall architecture within seconds of exposure to osmotic stress. The prevailing view is that resistance to osmotic stress is dependent upon key signaling pathways that mediate osmohomeostasis (45, 46). Early studies on the response of *Saccharomyces cerevisiae* to osmotic stress indicated that loss of viability is related to the loss of cell volume and that osmotically challenged cells display cell wall alterations and cytoskeleton reorganization (47, 48). More-recent reports on the biophysical responses of *S. cerevisiae* cells to osmotic stress indicate a direct relationship between loss of turgor pressure and Hog1 pathway activation and suggest that the extent of Hog1 pathway activation is directly linked to the mechanical properties of the membrane (49). Interestingly, those authors predicted that the yeast cell wall might be elastic because the cell wall was observed to follow the plasma membrane as it shrinks during osmotic shock. Similarly, hyperosmotic stress activates the Hog1 mitogen-activated protein kinase (MAPK) pathway in *C. albicans*. This induces glycerol biosynthetic gene expression, the intracellular ac-

cumulation of this osmolyte, the restoration of turgor pressure, and, ultimately, the resumption of growth (45, 46, 50–54). Meanwhile, the Cek1 and Mkc1 MAPK pathways modulate cell wall biosynthesis in response to hyperosmotic stress, thereby contributing to osmoadaptation (53, 55–57). However, the relationship between osmotic stress resistance and cell wall structure is unclear, and the role of the fungal cell wall in mediating osmotic stress resistance remains largely unexplored.

While MAPK signaling pathways, in particular, the Hog1 pathway, are important for osmoadaptation in *C. albicans*, we show that they are not essential for survival immediately following exposure to acute osmotic stress. Those *C. albicans* cells that are killed by osmotic stress die within minutes of exposure, before Hog1 or Mkc1 signaling can mediate the changes in expression and the osmolyte accumulation that are required for longer-term adaptation to hyperosmotic stress. We found that cellular survival during this critical early phase is dependent on cell wall elasticity and on the degree to which this elasticity can buffer sudden changes in cell volume. Our observations reveal a surprisingly high level of dynamism for the “rigid” fungal cell wall.

RESULTS

The ability to survive hyperosmotic stress is not dependent on Hog1 signaling or glycerol accumulation. Previously, we showed that *C. albicans* cells grown on physiologically relevant alternative carbon sources, such as the carboxylic acid lactate, display enhanced survival following exposure to osmotic stress compared with cells grown on glucose (58). Therefore, we tested whether this enhanced osmotic stress resistance is dependent upon key signaling pathways that mediate adaptation to hyperosmotic shock. First, we examined Hog1 signaling, which is essential for osmoadaptation (45, 46, 50–54). Interestingly, the inactivation of Hog1 did not reduce the survival of glucose- or lactate-grown *C. albicans* cells following NaCl treatment (Fig. 1A), even though these *hog1* Δ cells displayed attenuated growth on NaCl-containing medium irrespective of the carbon source they were grown on (see Fig. S1 in the supplemental material), as expected (50, 51).

The enhanced hyperosmotic stress survival of lactate-grown cells was not reduced in *hog1* Δ cells (Fig. 1A), which was consistent with our previous findings (58). Therefore, we compared the dynamics of Hog1 activation in lactate- and glucose-grown cells following hyperosmotic shock. Glucose-grown cells displayed rapid and sustained Hog1 phosphorylation following exposure to 1 M NaCl (Fig. 1B), which recapitulated previous observations (51, 59–61). In contrast, Hog1 phosphorylation levels were relatively high in unstressed lactate-grown cells, and they declined after hyperosmotic shock (Fig. 1B). Consistent with these observations, osmotic stress did not stimulate the nuclear localization of Hog1 in lactate-grown cells (Fig. 1C), whereas Hog1 accumulated in the nucleus of glucose-grown cells, as expected (45).

Next, we examined glycerol accumulation in lactate-grown *C. albicans* cells. As expected (50, 61), glucose-grown cells accumulated intracellular glycerol after exposure to 1 M NaCl, and this was blocked in *hog1* Δ cells (Fig. 1D). In contrast, wild-type lactate-grown cells did not accumulate glycerol in response to NaCl treatment (Fig. 1D). We conclude that while Hog1 signaling is clearly required for osmoadaptation, the survival of *C. albicans* cells after hyperosmotic shock is not dependent on Hog1 signaling or glycerol accumulation.

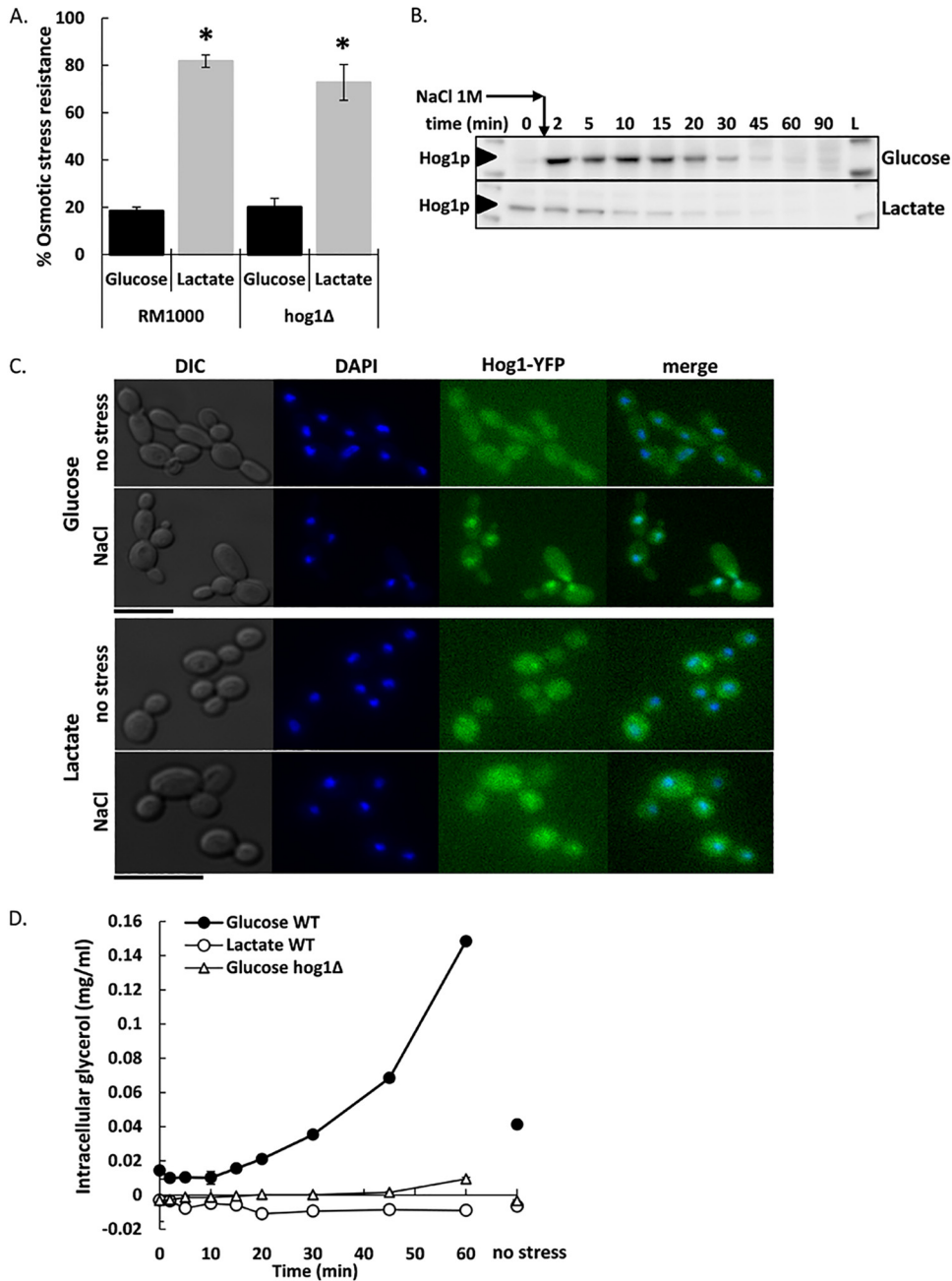


FIG 1 Hog1 accumulation and glycerol accumulation do not mediate the enhanced osmotic stress resistance of lactate-grown cells. (A) Viability of wild-type (RM1000) and *hog1Δ* cells grown on glucose or lactate 1 h after exposure to hyperosmotic stress (2 M NaCl) as determined by percent CFU (colony forming units) relative to untreated controls. (B) Western blots of Hog1 phosphorylation in lactate- and glucose-grown wild-type cells after imposition of osmotic stress (1 M NaCl). L, marker lane. (C) Hog1 localization in lactate- and glucose-grown cells using a Hog1-YFP (green)-tagged strain and DAPI nuclear staining (blue) 10 min following exposure to osmotic stress (1 M NaCl). Bars = 5 μm. DIC, differential interference contrast. (D) Glycerol accumulation in wild-type glucose- and lactate-grown cells and in *hog1Δ* glucose-grown cells following exposure to osmotic stress (1 M NaCl). Intracellular glycerol levels in non-stressed control cells are indicated on the right side of the graph.

Enhanced osmotic stress survival is not dependent on Cek1 or Mkc1 signaling. Cek1 signaling also contributes to osmoadaptation (56, 57), and therefore we tested whether this pathway contributes to the survival of *C. albicans* cells following hyperosmotic shock. We also examined Mkc1, the *C. albicans* MAP kinase on the cell wall integrity pathway (62). Neither the inactivation of Cek1 nor the inactivation of Mkc1 affected the survival of glucose- or

lactate-grown cells after NaCl treatment. Furthermore, the enhanced osmotic stress survival of lactate-grown cells was not attenuated in *cek1Δ* or *mkc1Δ* cells (Fig. 2A). Also, neither Cek1 nor Mkc1 was strongly phosphorylated following the imposition of hyperosmotic stress on wild-type *C. albicans* cells grown on lactate (Fig. 2B). Therefore, the Cek1 and Mkc1 signaling pathways are not required for the survival of *C. albicans* cells following hyperosmotic shock.

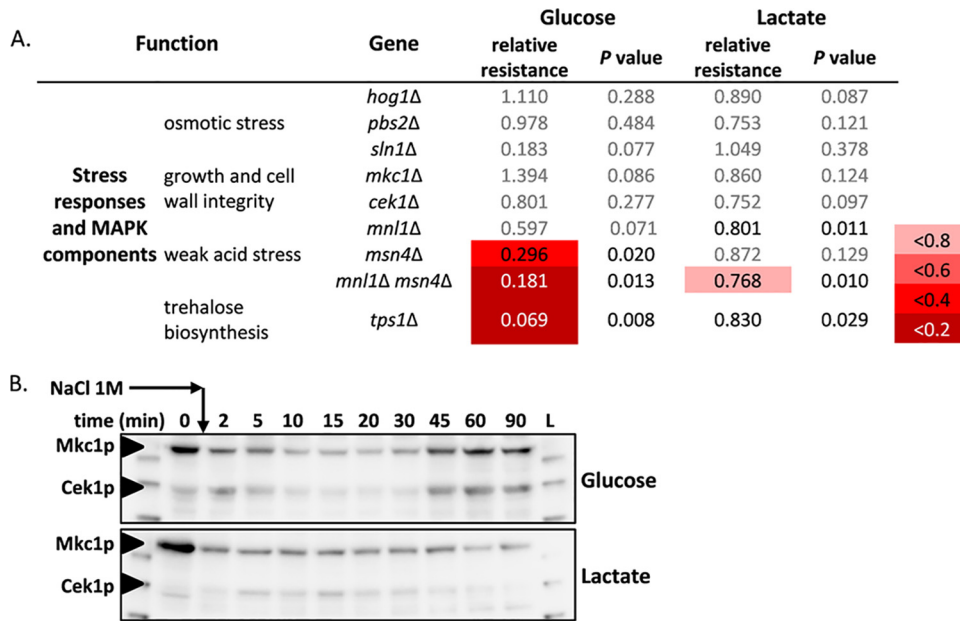


FIG 2 MAPK signaling pathways and other stress regulators do not mediate the high osmotic stress resistance of lactate-grown cells. (A) Mutant screen in which components of MAPK and stress signaling pathways were tested for their contributions to osmotic stress resistance following exposure to 2 M NaCl for 1 h. Relative resistance levels are shown as the ratios between the resistance of the mutant strain and that of the wild-type parental control. Boxes are colored pale red (relatively small impact on stress resistance) to dark red (relatively large impact) according to the scale on the right. (B) Western blots of Mkc1 and Cek1 phosphorylation in lactate- and glucose-grown cells under conditions of osmotic stress (1 M NaCl).

Cell death occurs within minutes of an acute hyperosmotic shock. The observations reported above indicated that MAP kinase-mediated adaptation mechanisms are not essential for cell survival following osmotic stress. Therefore, we examined the dynamics of cell killing following exposure to hyperosmotic stress. Interestingly, most of the killing occurred within 5 to 10 min of exposure to salt (Fig. 3A), before Hog1-mediated glycerol accumulation had begun (Fig. 1D).

We reported previously that lactate-grown *C. albicans* cells display slower volumetric changes than glucose-grown cells follow-

ing the imposition of an osmotic stress (58). Therefore, using microfluidics, we examined in more detail the dynamics of cell volume changes in the 10 min following exposure of cells to 1 M NaCl (Fig. 3B). The cell volume of glucose-grown cells decreased rapidly, within 30 to 60 s of salt addition, and this volume did not recover within the 10-min period examined, probably because most cells were no longer viable (Fig. 3A). Lactate-grown cells also lost volume, but the decline was less abrupt, and their volume was partially restored within 3 min. Hog1 inactivation exerted minimal effects on cell volume dynamics (Fig. 3B), consistent with the

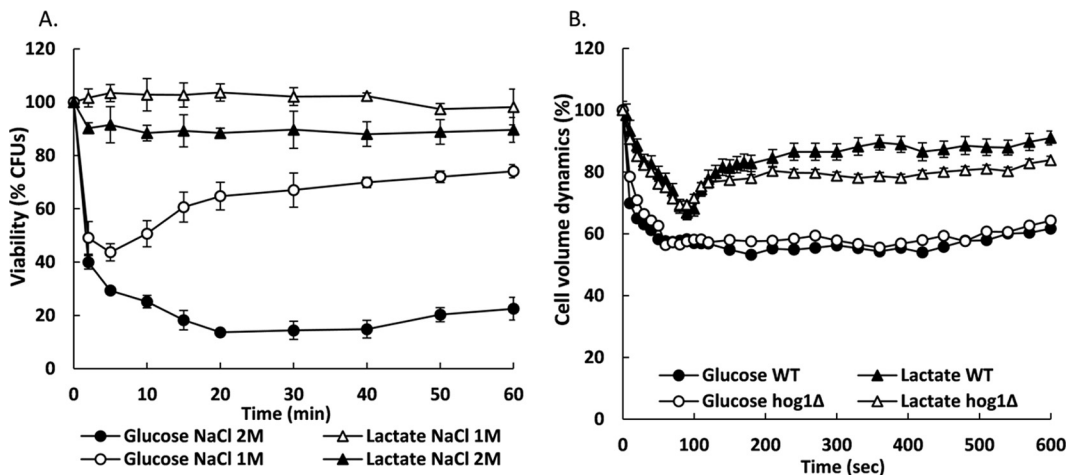


FIG 3 The initial events during osmoadaptation are critical for cell survival. (A) Cell death of lactate- and glucose-grown *C. albicans* cells after exposure to hyperosmotic stress (1 M and 2 M NaCl). Resistance levels are expressed as percent CFU relative to the initial number of CFU. (B) Cell volume dynamics of lactate- and glucose-grown *C. albicans* wild-type (WT) and *hog1Δ* cells after addition of osmotic stress (1 M NaCl). Deletion of *HOG1* did not significantly affect the initial volumetric transitions in the first 10 min of exposure to osmotic stress.

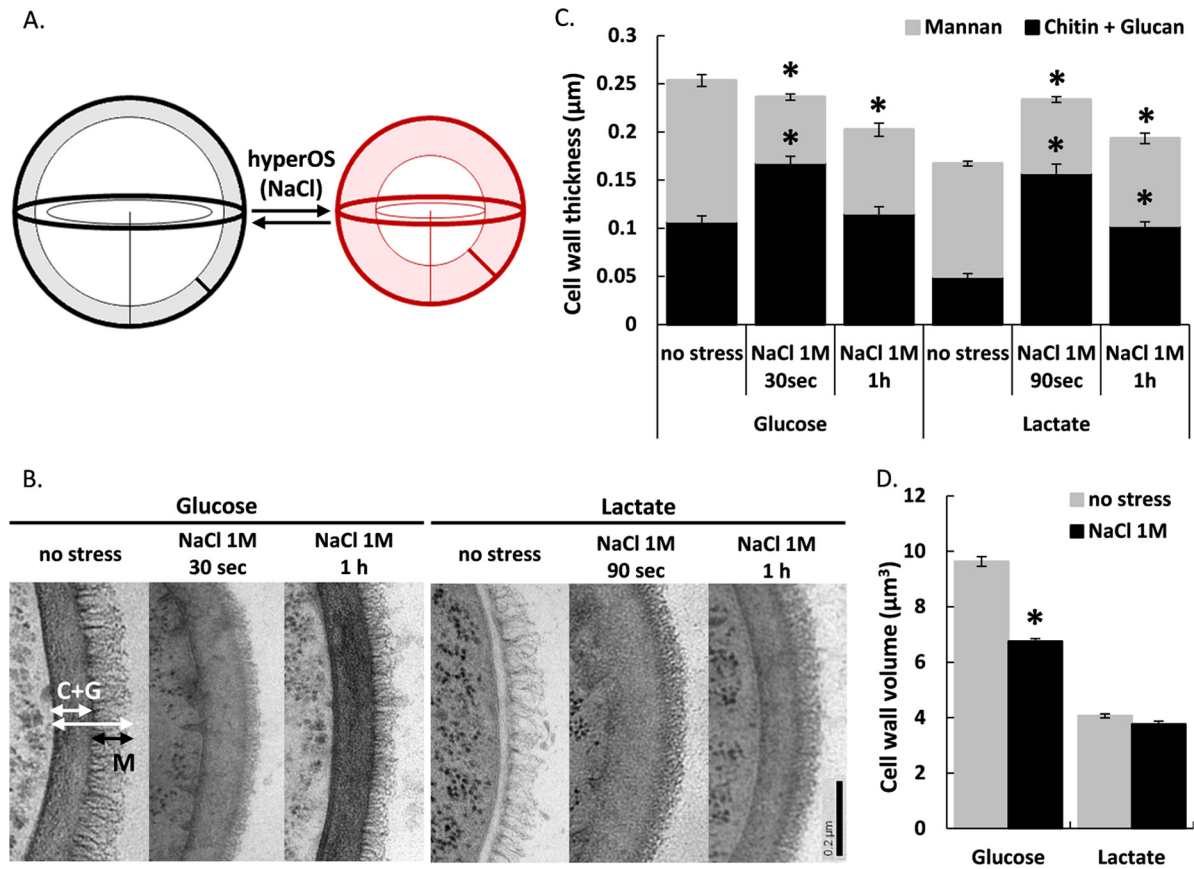


FIG 4 Dynamic changes in *C. albicans* cell wall architecture following hyperosmotic stress. (A) Predicted changes in cell wall thickness following changes in cell volume after exposure to hyperosmotic stress (hyperOS). (B) TEM images of cell walls from *C. albicans* cells grown on glucose or lactate and exposed to osmotic stress (1 M NaCl) for the specified time (representative images from ~100 cells imaged). Bar, 0.2 µm. The 30 s and 90 s time points were chosen based on when the maximum volumetric changes were observed (Fig. 3B). G+C, β-glucan and chitin; M, mannan. (C) Quantification of cell wall thickness based on TEM pictures ($n > 50$ cells). (D) Quantification of total cell wall volume of glucose-grown cells (at 30 s) and lactate-grown cells (at 90 s) after exposure to 1 M NaCl relative to the no-stress controls. Cell wall volumes were calculated based on TEM images and microfluidic volumetric measurements of total cell volume.

observation that *hog1Δ* cells do not display attenuated survival (Fig. 1A). The differences between lactate- and glucose-grown cells were even more apparent following exposure to high-salt conditions (2 M NaCl; see Fig. S2 in the supplemental material).

Rapid cell wall remodeling accompanies cell volume changes during osmotic stress. We reasoned that the rapid changes in cell volume during hyperosmotic shock are likely to be accompanied by significant changes to the cell wall. If one assumes that the cell wall biomass does not change significantly within 30 to 60 s, then this biomass must become distributed over a surface area when the cell volume decreases. In other words, the β-glucan–chitin layer of the wall is likely to become thicker (Fig. 4A). We tested this by comparing the cell walls of glucose- and lactate-grown cells before salt addition, at the points of maximum volume loss (30 and 90 s, respectively), and after osmoadaptation (1 h) using high-pressure freeze substitution transmission electron microscopy (HPF-TEM). This analysis revealed dramatic changes in cell wall architecture immediately following salt exposure for both glucose- and lactate-grown cells (Fig. 4B). Concomitant with the loss in cell volume, there was a significant increase in the diameter of the inner β-glucan and chitin layer of the cell wall (Fig. 4C). Meanwhile, the external fibrillar layer of mannoproteins became narrower and more dense (Fig. 4B and C). This high degree of cell

wall reorganization was particularly dramatic for lactate-grown cells, where the inner cell wall thickness increased more than 3-fold within 90 s (Fig. 4C). The changes in cell wall thickness were reversible, their diameters partially returning to normal after 1 h (Fig. 4B and C). This seems analogous to a spring being compressed and relaxed. Volumetric analyses also revealed that, unlike the cell walls of lactate-grown cells, the walls of glucose-grown cells significantly decreased in thickness under conditions of osmotic stress, reflecting further differences in the ways that lactate- and glucose-grown cells deal with osmotic insults (Fig. 4D).

We tested whether the extreme elasticity of the *C. albicans* cell wall was triggered by salt rather than hyperosmotic shock by performing analogous experiments with 2 M and 4 M sorbitol. Sorbitol yielded observations similar to those seen with NaCl (see Fig. S3 in the supplemental material). Lactate-grown cells were more resistant to high concentrations of sorbitol than glucose-grown cells (see Fig. S3A), with most killing occurring in the first minutes of exposure to the stress (see Fig. S3B). Glucose-grown cells displayed more-dramatic decreases in volume than lactate-grown cells (see Fig. S3C). Also, significant increases in cell wall thickness were observed for lactate-grown cells (see Fig. S3D and E). We conclude that the *C. albicans* cell wall is extremely dy-

Function	Strain	Glucose		Lactate		
		relative resistance	P value	relative resistance	P value	
chitin synthase	<i>chs3Δ</i>	1.028	0.476	0.789	0.024	
β-1,3-glucan synthase	<i>fks1Δ</i>	0.418	0.047	0.900	0.048	
β-1,3-glucanosyltransferase	<i>pga4Δ</i>	0.341	0.029	0.883	0.176	
β-1,3-glucanosyltransferase	<i>phr1Δ</i>	0.740	0.085	0.694	0.036	
β-1,3-glucanosyltransferase	<i>phr2Δ</i>	0.628	0.103	0.844	0.035	
β-1,3-glucan cross-linking protein	<i>pir1Δ</i>	0.686	0.104	0.636	0.040	>4
β-glucan associated cell wall protein	<i>ssr1Δ</i>	0.410	0.017	0.826	0.134	>3
glucan-chitin cross-linker, predicted transglycosylase	<i>crh11Δ</i>	0.394	0.003	0.715	0.012	>2
cell wall protein, CRH family member	<i>crh12Δ</i>	0.529	0.055	0.447	0.002	>1.75
glycosidase, predicted glucan-chitin cross-linker	<i>utr2Δ</i>	0.664	0.046	0.351	<0.001	>1.5
CRH gene family	<i>crh11Δ</i>	1.025	0.454	0.138	<0.001	>1.25
	<i>crh12Δ utr2Δ</i>					<0.8
						<0.6
						<0.4
						<0.2

Function	Gene	Glucose		Lactate		
		+/- dox relative resistance	P value	+/- dox relative resistance	P value	
glucosyltransferase	<i>BGL2</i>	1.551	0.032	1.135	0.169	
chitinase	<i>CHT1</i>	0.617	0.038	1.176	0.051	
activator of Chs3p chitin synthase;	<i>CHS4</i>	1.035	0.432	1.167	0.129	
β-1,3-glucanosyltransferase	<i>PHR1</i>	1.356	0.044	1.235	0.017	>4
β-1,3-glucanosyltransferase	<i>PHR2</i>	0.906	0.416	1.243	0.039	>3
β-1,3-glucanosyltransferase	<i>PIR1</i>	1.084	0.389	1.245	0.041	>2
β-glucan associated cell wall protein	<i>SSR1</i>	2.446	0.033	1.069	0.244	>1.75
glucan-chitin cross-linker, predicted transglycosylase	<i>CRH11</i>	4.921	<0.001	1.231	0.109	>1.5
glycosidase, predicted glucan-chitin cross-linker	<i>UTR2</i>	2.565	0.004	1.341	0.032	>1.25
						<0.8
						<0.6
						<0.4
						<0.2

FIG 5 Genetic screen for changes in osmotic stress resistance of *C. albicans* strains with altered expression levels of cell wall components. *C. albicans* strains (see Table S1 in the supplemental material) either lacking (A) or overexpressing (B) different cell wall structural components were tested for their resistance to 2 M NaCl (1 h exposure). In panel A, relative resistance levels are expressed as the fold ratio between the osmotic stress resistance of a null mutant and that of its wild-type parental control under equivalent conditions. In panel B, the relative resistance of a *tetON* overexpression mutant is expressed as the ratio of the levels of osmotic stress resistance in the presence and absence of doxycycline. Boxes are colored dark green (where the mutation leads to a large increase in osmotic stress resistance) to red (where the mutation decreases osmotic stress resistance) according to the scale on the right.

dynamic, displaying an ability to readjust its architecture within seconds of exposure to hyperosmotic shock (Fig. 4A).

Cell wall remodeling enzymes influence osmotic stress resistance. The osmotic stress resistance of *C. albicans* cells and the elasticity of their cell walls are strongly influenced by the growth conditions (Fig. 1 and 3; see also Fig. S3 in the supplemental material) (58). These growth conditions also influence the expression of cell wall carbohydrate active enzymes such as Cht1, Phr1, and Phr2 that are involved in cell wall cross-linking (40). Therefore, we reasoned that the degree of cross-linking in the β-glucan–chitin network is likely to influence cell wall elasticity, which, in turn, affects cell survival following hyperosmotic stress. According to this working hypothesis, a stiffer cell wall constrains the rate of change in cell volume, thereby decreasing the likelihood that a hyperosmotic shock will compromise cell integrity, for example, by rupturing the plasma membrane.

To test this, we examined the sensitivity of various glucose- or lactate-grown *C. albicans* cell wall mutants to NaCl. The cells included null and overexpression mutants of glucanosyltransferases (Pga4, Phr1, and Phr2), the Crh family of putative cell wall transglycosylases involved in linking chitin to β-glucan (Utr2, Crh11, and Crh12) (32), a chitin synthase (Chs3), the catalytic subunit of β-glucan synthase (Fks1), and β-glucan-linked cell wall proteins (Pir1 and Ssr1) (63–65). The inactivation of any single gene exerted relatively minor effects upon the osmotic stress resistance of glucose- and lactate-grown *C. albicans* cells (Fig. 5A). Interestingly, a triple *crh11Δ crh12Δ utr2Δ* mutation dramatically attenuated the osmotic stress resistance of lactate-grown *C. albicans* cells. In contrast, overexpression of *CRH11*, *UTR2*, and *SSR1* increased the osmotic stress resistance of glucose-grown cells (Fig. 5B). These observations suggest that the frequency of β-glucan–chitin cross-links in the

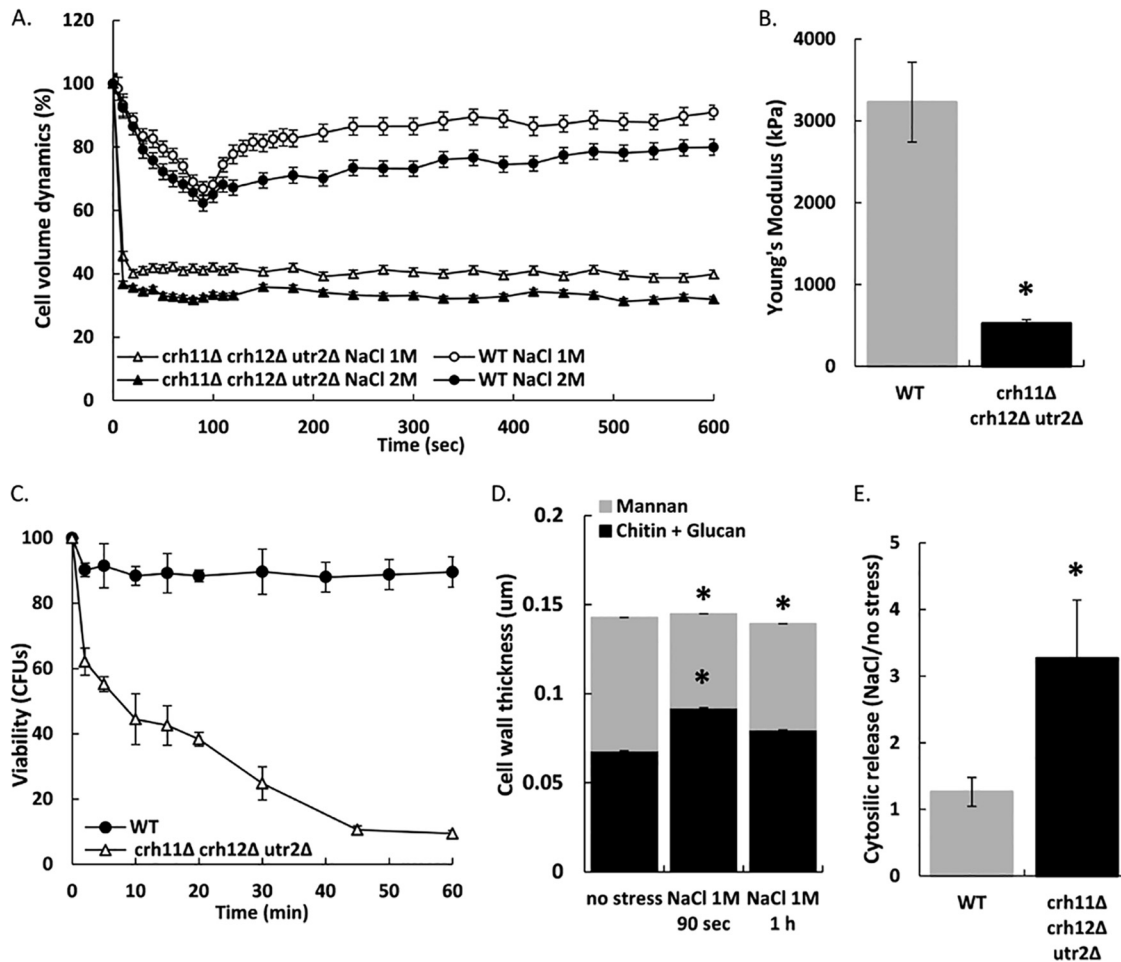


FIG 6 The *CRH* family of cell wall proteins is critical for osmotic stress resistance of lactate-grown cells. (A) Cell volume dynamics following exposure to either 1 M or 2 M NaCl for lactate-grown wild-type or *crh11Δ crh12Δ utr2Δ* mutant cells. (B) Comparison of the levels of elasticity of lactate-grown wild-type and *crh11Δ crh12Δ utr2Δ* mutant cells by atomic force microscopy. (C) Cell death following osmotic stress for lactate-grown *crh11Δ crh12Δ utr2Δ* and wild-type cells after exposure to 2 M NaCl. Resistance levels are expressed as percent CFU relative to the initial number of CFU. (D) Cell wall thickness of lactate-grown *crh11Δ crh12Δ utr2Δ* cells under conditions of osmotic stress (1 M NaCl) based on TEM pictures ($n > 50$ cells) at the specified time points and compared to untreated control cells. (E) Cytosolic release (A_{260}) was measured 10 min after exposure to 2 M NaCl for wild-type and *crh11Δ crh12Δ utr2Δ* cells grown on lactate. The data represent the ratios between osmotically shocked and untreated cells averaged from the results from 3 independent experiments \pm SEM.

cell wall influences the osmotic stress resistance of *C. albicans* cells.

The *CRH* family modulates osmotic stress resistance by controlling cell wall elasticity. We hypothesized that cell wall transglycosylases may exert their effects upon osmotic stress resistance by altering cell wall elasticity. To test this, we examined the effects of inactivating *CRH11*, *CRH12*, and *UTR2* on the behavior of lactate-grown *C. albicans* cells during hyperosmotic shock (Fig. 6). Lactate-grown wild-type cells decreased in volume relatively slowly over a 90-s period before recovering some of their volume. The thickness of the β -glucan–chitin layer in their cell walls increased over this time scale (Fig. 4C), and about 90% of these cells survived a hyperosmotic shock. In contrast, following NaCl addition, the lactate-grown *crh11Δ crh12Δ utr2Δ* triple mutant almost instantaneously lost \sim 60% of its cell volume and failed to restore this volume over time (Fig. 6A). Consistent with our hypothesis, atomic force microscopy (AFM) measurements of wild-type and *crh11Δ crh12Δ utr2Δ* cells revealed a dramatic increase in cell wall elasticity for the triple mutant, as shown by a decreased Young's

modulus (Fig. 6B). More than half of these mutant cells were dead within 10 min of exposure to salt (Fig. 6C). After 90 s, the β -glucan–chitin layer of the *crh11Δ crh12Δ utr2Δ* cells was only slightly thicker than that of untreated control cells (Fig. 6D), consistent with the hypothesis that the cell wall of the triple mutant is architecturally different. We reasoned that this abnormally elastic cell wall might be less able to protect the plasma membrane against the sudden volumetric changes imposed by the osmotic stress, leading to cell lysis. This hypothesis was supported by the release of cytoplasmic contents, reflected in the increased absorbance of supernatants at 260 nm when the triple mutant was challenged with hyperosmotic stress (Fig. 6E). We conclude that the loss of Crh cross-linking enzymes increases the elasticity of *C. albicans* cell walls and hence their vulnerability to hyperosmotic stress.

We tested these ideas further by overexpressing the cell wall cross-linking enzymes *Utr2* and *Crh11* (see Fig. S5 in the supplemental material). On the basis of the observations reported above, the doxycycline-conditional induction of *tetON-UTR2* or *tetON-CRH11* was expected to reduce the elasticity of glucose-grown

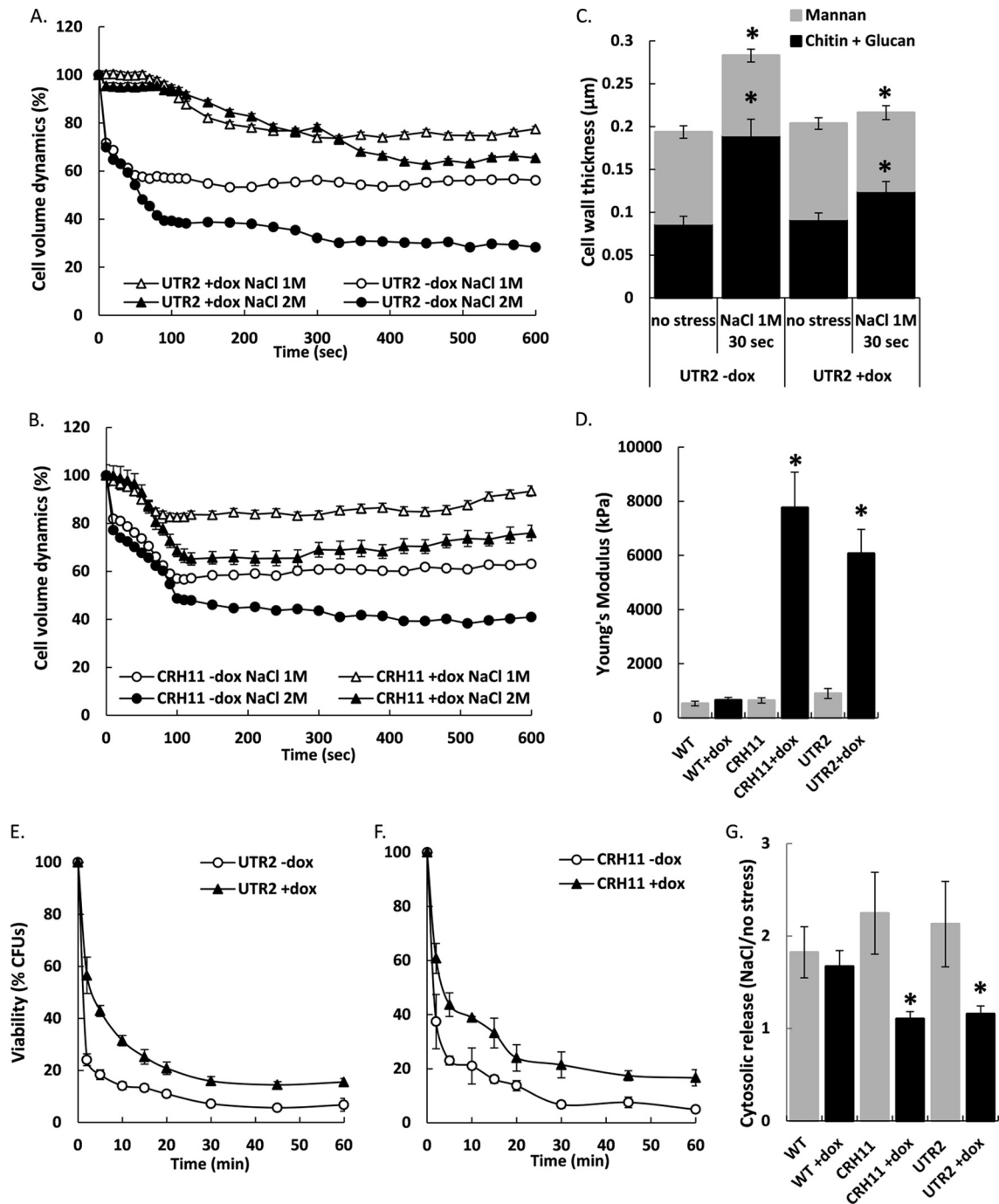


FIG 7 Overexpression of *CRH11* or *UTR2* results in reduced cell wall elasticity and delays cell death following hyperosmotic stress in glucose-grown cells. (A and B) Cell volume dynamics following exposure to 1 M or 2 M NaCl for glucose-grown *tetON-UTR2* (A) or *tetON-CRH11* (B) cells in the presence or absence of doxycycline (dox). (C) Cell wall thickness of glucose-grown *tetON-UTR2* cells (\pm doxycycline) after addition of 1 M NaCl, based on TEM pictures ($n > 50$ cells) at the specified time points. (D) Cell wall elasticity of glucose-grown wild-type, *tetON-UTR2*, and *tetON-CRH11* cells (\pm doxycycline) as determined by atomic force microscopy. (E and F) Viability of glucose-grown *tetON-UTR2* (E) or *tetON-CRH11* (F) cells (\pm doxycycline) following exposure to 2 M NaCl. Viability is expressed as percent CFU relative to the initial number of CFU ($t = 0$). (G) Cytosolic release (A_{260}) of culture supernatants 10 min after exposure to 2 M NaCl for glucose-grown wild-type, *tetON-UTR2*, and *tetON-CRH11* cells (\pm doxycycline). Data represent the ratios between osmotically shocked and untreated cells in 3 independent experiments (means \pm SEM).

cells and hence to protect these cells against hyperosmotic shock. As predicted, the overexpression of either *UTR2* or *CRH11* significantly decreased the volumetric changes observed for glucose-grown cells following NaCl addition (Fig. 7A and B). The over-

pressing cells lost less volume than the control cells lacking doxycycline. Doxycycline treatment alone had no effect on cell volume dynamics under conditions of osmotic stress (see Fig. S4). The reduced dynamism of cell volumetric changes correlated with

less-dramatic changes in the cell wall volume for *UTR2*-overexpressing cells after 30 s of NaCl treatment (Fig. 7C). Significantly, atomic force microscopy directly confirmed that *UTR2* and *CRH11* overexpression reduced the elasticity of the cell wall (Fig. 7D). Furthermore, *UTR2* and *CRH11* overexpression provided some degree of protection against hyperosmotic shock (Fig. 7E and F). Neither *UTR2* overexpression nor *CRH11* overexpression during growth on glucose was sufficient to confer the high levels of hyperosmotic shock resistance observed for lactate-grown cells, suggesting that survival under these conditions is a polygenic trait. Nevertheless, significant decreases in cell lysis were observed for the *UTR2*- and *CRH11*-overexpressing mutants (Fig. 7G).

The decrease in cell wall elasticity mediated by *UTR2* and *CRH11* overexpression was further confirmed by examining the impact of hypo-osmotic shock on cell volume. *UTR2* overexpression significantly reduced the extent to which H₂O addition induced an increase in the volume of glucose-grown *C. albicans* cells (see Fig. S6F in the supplemental material). Taken together, these observations suggest that modulating the levels of Crh cell wall cross-linking enzymes affects cell wall elasticity, which, in turn, impacts cell wall dynamics and cell survival during hyperosmotic insults.

Calcineurin signaling regulates carbon source-induced cell wall remodeling. Our data indicate that the architectural and elasticity characteristics of the cell wall differ significantly for glucose- and lactate-grown cells. They also show that these differences affect the ability of *C. albicans* cells to withstand hyperosmotic shock. This raised the issue of the speed with which the *C. albicans* cell wall undergoes transitions between these states, namely, for the relatively elastic wall of glucose-grown cells and the stiffer wall of lactate-grown cells. To test this, we examined the temporal changes in resistance to hyperosmotic shock at various times after *C. albicans* cells were transferred from glucose- to lactate-containing media and vice versa. As controls, we also monitored cells that were transferred from glucose to glucose and from lactate to lactate.

Control cells were grown on glucose or lactate and then transferred to fresh media containing the same carbon source. These cells maintained relatively constant levels of osmotic stress resistance throughout the experiment: glucose-grown cells remained relatively sensitive, and lactate-grown cells maintained their high resistance to NaCl exposure (Fig. 8A). Following their transfer to glucose medium, lactate-grown cells gradually lost their resistance over 3 h. Meanwhile, glucose-grown cells acquired osmotic stress resistance within 1 h of transfer to lactate medium (Fig. 8A). These transitions were slow compared to the rapid changes in cell wall architecture that occur following hyperosmotic shock, and hence the transition from one preadapted state to the other may require new cell wall synthesis. However, these timescales do not simply correlate with the growth rates on these carbon sources: the populations of these *C. albicans* cells double every 50 min on glucose and every 230 min on lactate (58). Therefore, these transitions may also involve the differential regulation of cell wall cross-linking enzymes (40).

The expression of *UTR2* and *CRH11* in *C. albicans* is regulated by calcineurin, an Ca²⁺-calmodulin-dependent serine/threonine protein phosphatase that is involved in maintaining cell wall integrity and stress responses (32, 66). Therefore, we tested whether calcineurin is required for the transition from osmotic stress-

sensitive glucose-grown cells to osmotic stress-resistant lactate-grown cells. Once again, wild-type cells became resistant to osmotic stress within 1 h of transfer to lactate medium (Fig. 8B). However, *cna1*Δ cells, which lack the catalytic subunit of calcineurin (66), did not become resistant to osmotic stress over this period. They remained relatively sensitive to 2 M NaCl. Furthermore, like *cna1*Δ cells, lactate-grown *crz1*Δ cells were sensitive to osmotic stress resistance relative to the wild-type control (Fig. 8C). *CRZ1* encodes a calcineurin-regulated transcription factor with key roles in cell wall remodeling (67, 68). These data suggest that the calcineurin pathway is a key modulator of *C. albicans* cell wall elasticity and that this modulation is partly achieved by controlling the expression of Crh transglycosylases.

DISCUSSION

The fungal cell wall is often viewed as a structurally rigid envelope that establishes cellular morphology (8, 13–15, 25). Indeed, cell wall polymers have been compared to reinforced concrete (69), and the impression of structural solidity has been strengthened by models that impute the formation of such structures to the rigidification of synthesized hyphal walls (34, 35, 70). Nevertheless, the molecular content of the cell wall is responsive to environmental change. Variations in nutrient availability, fluctuations in ambient pH and temperature, and antifungal drug treatments trigger changes in the expression of cell wall biosynthetic enzymes, structural proteins, and remodeling enzymes (37–44, 71). However, tens of minutes are required before these environmental inputs are manifested in newly synthesized cell wall and hence in cells with significantly altered properties (40, 58, 72) (Fig. 8 and 9). Here we describe a much higher degree of cell wall dynamism which permits major architectural alterations within seconds of a hyperosmotic shock (Fig. 4). NaCl or sorbitol treatment revealed this extreme elasticity by triggering dramatic changes in cell volume and, consequently, sudden changes in cell wall architecture (Fig. 3 and 4; see also Fig. S3 in the supplemental material).

These sudden changes in cell wall architecture occur within seconds of an osmotic shock. This truncated time scale suggests that these changes are mediated in response to rapid biophysical forces following the shock, rather than through adaptive changes in gene expression, which take tens of minutes to manifest themselves in a cell wall with altered properties (Fig. 8). Indeed, mutations that block Hog1 or Mkc1 signaling did not affect cell survival following acute hyperosmotic shock (Fig. 1 and 2) but the degree of cross-linking between cell wall polymers had a dramatic effect (Fig. 6 and 7).

Several factors appear to contribute to the elasticity of the *C. albicans* cell wall. The helical conformation of β-glucans in the yeast cell wall (73, 74) may permit their expansion and contraction in a manner analogous to that of a coiled spring (Fig. 9). Also, slippage of locally aligned polymers over one another could promote the rapid changes that are observed in the dimensions of the β-glucan–chitin layer in the cell wall. However, rates of β-glucan helical compression and slippage must be constrained by covalent cross-links to other cell wall polymers, for example, to other β-glucan molecules by the phr family and to chitin by Crh11, Crh12, and Utr2 enzymes (Fig. 9) (31, 32). In *S. cerevisiae*, Crh1 generates cross-links between β-1,6-glucan and chitin (29). However, Pardini and coworkers reported a decrease in levels of alkali-insoluble β-1,3-glucan (but not alkali-insoluble β-1,6-glucan) in *C. albicans* *crh11*Δ *crh12*Δ *utr2*Δ cells (31, 32). Nevertheless, they also

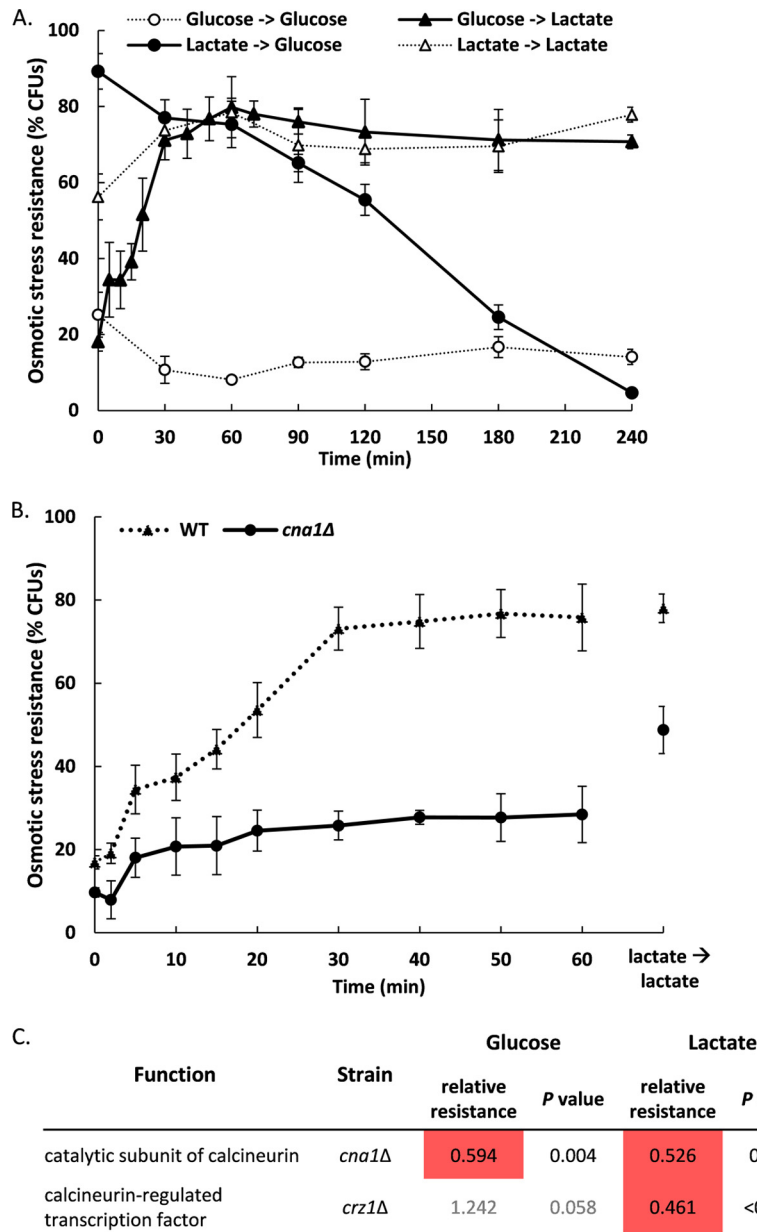


FIG 8 Calcineurin signaling regulates carbon source-induced cell wall remodeling. (A) To examine the transitions between two different cell wall states, wild-type *C. albicans* cells were transferred from one carbon source to another, and the effects on their osmotic stress resistance were measured every 30 min for 4 h. Control cells were transferred to the same carbon source (i.e., from lactate to lactate or from glucose to glucose). At each time point, cells were exposed to 2 M NaCl and then cell viability was measured (CFU). Resistance levels are expressed as percent CFU relative to the corresponding unstressed control. (B) The changes in osmotic stress resistance (2 M NaCl) observed for wild-type and *cna1Δ* (catalytic subunit of calcineurin) cells grown on glucose following their transfer to lactate media. Data representing the levels of osmotic stress resistance of cells grown on lactate and transferred to lactate are shown on the right side of the graph. (C) Levels of osmotic stress resistance of glucose- and lactate-grown mutants with defects in calcineurin (*cna1Δ*) or the calcineurin-regulated transcription factor (*crz1Δ*) relative to those seen with their wild-type controls. Relative resistance data represent the ratios between the resistance of the mutant and that of the corresponding wild-type control. Boxes are colored according to the scale on the right (with dark red reflecting a relatively large impact on stress resistance).

suggested that Mkc1 activation might lead to compensatory changes that reduce the impact of *UTR2* inactivation on linkages between β -1,6-glucan and chitin. Taken together, the data suggest that key cross-linking genes such as *CRH11*, *CRH12*, and *UTR2* influence the elasticity of the *C. albicans* cell wall (Fig. 5 to 7), probably by modulating chitin- β -glucan linkages. Nevertheless, enzymes other than those of the Crh family may also contribute to this cell wall remodeling.

The degree of cell wall elasticity affects the ability of *C. albicans* cells to survive an acute hyperosmotic shock (Fig. 3 and 4). Cells that display excessive cell wall elasticity are unable to survive such a shock. For example, most glucose-grown wild-type and *crh11Δ crh12Δ utr2Δ* triple-mutant cells are rapidly killed by 2 M NaCl, whereas over 90% of lactate-grown wild-type cells survive this insult (Fig. 1, 3, and 6). This correlates with the release of cytoplasmic contents by mutant cells following osmotic shock

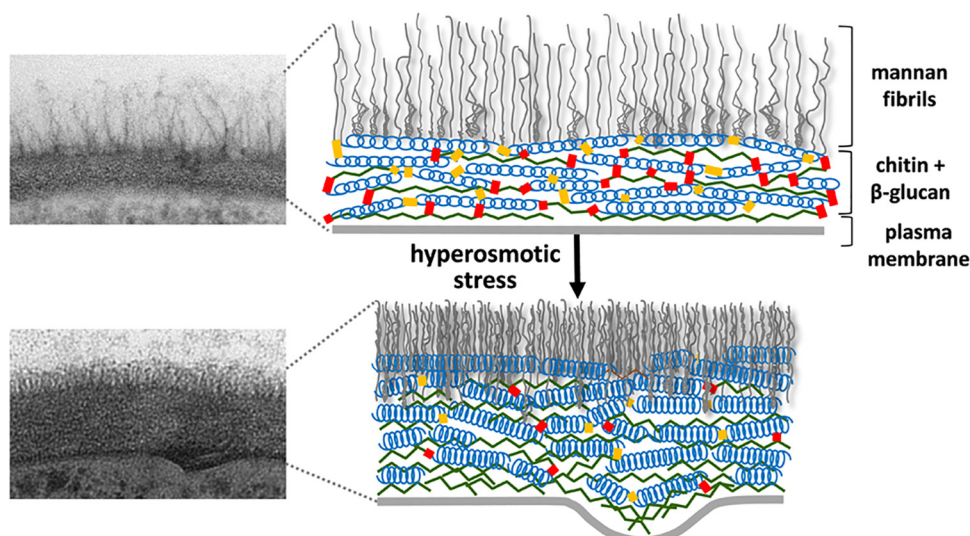


FIG 9 Model of cell wall plasticity and architectural changes occurring under conditions of hyperosmotic stress. TEM images of cell walls of unstressed cells (top) and cells immediately following hyperosmotic stress (bottom; 2 M NaCl) are shown on the left. Corresponding cartoons illustrating the possible structural changes are illustrated on the right as follows: plasma membrane, horizontal thick grey line; chitin chains, green lines; β -glucan coils, blue; mannan fibrils, horizontal grey lines; cross-links between β -glucan and chitin, red; cross-links between β -glucan coils, yellow. The rapid increase in cell wall thickness that follows hyperosmotic shock is predicted to involve compression of β -glucan coils and sliding of chitin and β -glucan polymers over one another. This is accompanied by invagination and, potentially, rupture of the plasma membrane (see the lower TEM panel).

(Fig. 6E). *UTR2* or *CRH11* overexpression reduces the elasticity of glucose-grown cells, providing them with some protection against this killing (Fig. 7). This highlights the key role for cell wall cross-linking enzymes in controlling the degree of cell wall elasticity and cellular robustness following osmotic shock. The reduced elasticity of lactate-grown cells, or of other cell types that express relatively high levels of cross-linking enzymes, leads to more-controlled changes in cell volume following an acute osmotic shock (Fig. 6 and 7). This correlates with reduced rates of cytoplasmic release (Fig. 6 and 7), suggesting that less-elastic cell walls protect the plasma membrane from rupture during acute osmotic shocks (Fig. 9), leading to increased resistance to the stress. The proportions of the major cell wall components are similar in glucose- and lactate-grown cells (58), but the differences in the cross-links in these cell walls are worthy of detailed biochemical characterization.

These observations raise several interesting issues. First, the *C. albicans* cell wall must have evolved sufficient elasticity to permit survival following hyper- or hypo-osmotic challenges (see, e.g., Fig. S6 in the supplemental material) while retaining sufficient rigidity to maintain cell morphology under these conditions. In this regard, it is intriguing that Hog1 signaling influences *C. albicans* morphology and cell wall robustness, as well as mediating osmoadaptation (50, 51, 59, 75–77). This must depend on tight regulation of both the synthesis and cross-linking of cell wall chitin, β -1,3-glucan, and β -1,6-glucan.

Second, the degrees of cell wall plasticity are likely to differ significantly for *C. albicans* cells colonizing the skin, oral cavity, gastrointestinal and urogenital tracts, or internal organs. This presumption is based on the differing nutrient availabilities in these host niches (78, 79) and the significant impact of physiologically relevant environmental inputs upon the expression of key cell wall cross-linking enzymes (39, 41, 58). Indeed, *C. albicans* mutants with defects in specific cell wall cross-linking enzymes display

niche-specific virulence defects (6, 80, 81). Similarly, cells that are unable to induce signaling pathways that regulate the expression of cell wall cross-linking proteins are also unable to mount full virulence (32, 66). Therefore, differential levels of cell wall elasticity might influence the fitness of *C. albicans* and hence its ability to colonize certain host niches.

In conclusion, the *C. albicans* cell wall displays a high degree of biophysical and biochemical flexibility (Fig. 4, 8, and 9) which influences its ability to survive acute osmotic challenges. The degree of cell wall elasticity is influenced by the levels of key cell wall remodeling enzymes, which are modulated by the available nutrients, suggesting that the osmotic stress resistance and stress adaptation characteristics of this pathogen differ between host niches. These observations have general applicability across the fungal kingdom.

MATERIALS AND METHODS

Strains and growth conditions. The *C. albicans* strains used in this study are listed in Table S1 in the supplemental material (88–99). All strains were grown at 30°C in minimal medium containing 0.67% yeast nitrogen base without amino acids (YNB) and 2% carbon source (glucose or sodium lactate) at pH 5.2 to 5.6 and were supplemented with the appropriate auxotrophic requirements at 10 μ g/ml (58). For analyses and stress assays, *C. albicans* cells were grown overnight at 30°C, diluted to an optical density at 600 nm (OD_{600}) of 0.1 in fresh medium, and regrown to the mid-exponential phase ($OD_{600} = 0.5$). For overexpressing strains, doxycycline was added to the growth medium for overnight and exponential-phase cultures (final concentration, 50 μ g/ml).

Strain construction. The doxycycline-conditional *BGL2*, *CHT1*, *CRH11*, *CHS4*, *PHR1*, *PHR2*, *PIR1*, *SSR1*, and *UTR2* overexpression strains were constructed as previously described (82) using the plasmids listed in Table S2 in the supplemental material. These overexpression plasmids were constructed using a Gateway cloning system (82), linearized with *Stu*I, and transformed into *C. albicans* strain CEC2175, selecting for uridine prototrophy. Correct integration at the *RPS1* locus was confirmed by diagnostic PCR (83).

HPF-TEM. High-pressure freeze substitution transmission electron microscopy (HPF-TEM) was performed as described previously (5, 58), including cutting ultrathin sections of 100 nm in thickness. All samples were imaged with a Philips CM10 transmission microscope (FEI, United Kingdom) equipped with a Gatan Bioscan 792 camera, and images were recorded using a Digital Micrograph (Gatan, Abingdon Oxon, United Kingdom). The thicknesses of the chitin- β -glucan and the mannan cell wall layers were measured by averaging >20 measurements for each cell ($n > 30$ cells) using Image-J.

Western blotting. Total soluble protein was extracted for Western blotting from mid-exponential-phase *C. albicans* cells grown on either glucose or lactate as previously described (51, 58). Hog1 activation was detected using phosphospecific phospho-p38 MAPK (Thr180/Tyr182) antibody 9211 (New England Biolabs, Hitchin, United Kingdom), while Mkc1 activation and Cek1 activation were detected using phosphospecific phospho-p44/42 MAPK (extracellular signal-regulated kinase-1/extracellular signal-regulated kinase-2 [ERK1/2]; Thr202/Tyr204) antibody 4370 (New England Biolabs). The secondary antibody was horseradish peroxidase (HRP)-labeled anti-rabbit IgG 7074 (New England Biolabs) and was detected using Pierce ECL Plus Western blotting reagents per the instructions of the manufacturer (Thermo Scientific, Cramlington, United Kingdom). Total protein levels were quantified using Bradford assays. Blots shown are representative of at least three biological replicates.

Osmotic stress resistance. To examine short-term resistance to hyperosmotic stress, mid-exponential-phase *C. albicans* cells were exposed to NaCl (1 M or 2 M) or sorbitol (2 M or 4 M) at 30°C for the indicated times, and cell viability (CFU) was measured relative to untreated control cells at $t = 0$. Means \pm standard errors of the means (SEM) of the results of at least four independent experiments are presented. To examine adaptation to hyperosmotic stress in the longer term, serial dilutions of mid-exponential-phase *C. albicans* cells were plated onto YNB agar containing the specified carbon source (glucose or lactate) plus NaCl (0, 0.5, or 1 M), starting with 5×10^7 cells per spot and diluting 1/10 thereafter. The plates were incubated for 2 to 4 days at 30°C and photographed. To examine resistance to hypo-osmotic stress, cultures of mid-exponential-phase *C. albicans* cells were diluted 2-fold in H₂O. Results shown are representative of data generated in at least three independent experiments, using more than 10^6 cells in each experiment.

Time-lapse volumetric analysis of *C. albicans* cells. An Onix microfluidic perfusion system (CellASIC Corp., USA) was used to analyze the dynamic volumetric responses of *C. albicans* cells to osmotic stress. Cells were grown to the mid-exponential phase at 30°C in either glucose or lactate YNB, and $\sim 5 \times 10^4$ cells were applied to Y04C microfluidic plates for each experiment. Growth medium was perfused at 30°C through a microfluidic chamber (3 mm by 3 mm) with ceiling heights of 3.5 μ m, 4.0 μ m, and 4.5 μ m and at a flow rate of 4 lb/in² (~ 10 μ l/h). After 5 min of preequilibration in the absence of stress, medium containing NaCl at the specified concentrations was perfused through the chamber. Cells were observed using a DeltaVision Core microscope (Image Solutions Ltd., Preston, United Kingdom), images were captured using a CoolSNAP camera (Photometrics United Kingdom Ltd., London, United Kingdom), and image analysis was performed using ImageJ v1.45 (<http://rsbweb.nih.gov/ij/>).

Hog1 localization. Exponentially growing *C. albicans* JC63 cells expressing Hog1-yellow fluorescent protein (YFP) were treated with hyperosmotic stress (1 M NaCl) for 10 min at 30°C, collected, fixed in 3.7% formaldehyde for 30 min, and compared to control unstressed cells. Cells were then centrifuged at 4,000 rpm for 5 min, washed three times in 2 ml PEM [1 mM MgSO₄, 1 mM EGTA, 0.1 M Na₂-PIPES [piperazine-N,N'-bis(2-ethanesulfonic acid)], pH 7.6], and resuspended in 100 μ l of PEM. Cells were prepared on poly-L-lysine-coated slides and stained with DAPI (4'-6'-diamidino-2-phenylindole) as described previously (45). Hog1-YFP localization was then examined using a DeltaVision Core microscope (Applied Precision, WA, USA), and the images were analyzed using Del-

taVision software (SoftWorx version 5.0.0). The images presented are representative of three independent replicate experiments.

Glycerol assays. Glycerol levels were assayed for wild-type (CAI4; see Table S1 in the supplemental material) and *hog1* Δ (JC45) cells exposed to stress for the specified times. Briefly, mid-exponential-phase cultures of *C. albicans* were subjected to hyperosmotic stress (0 or 1 M NaCl) and 1.5-ml samples collected for analysis. To measure extracellular glycerol, cells were first removed by centrifugation, and culture supernatants were then heated at 100°C for 10 min before analysis. For total glycerol determinations, 1.5 ml culture samples were heated at 100°C for 10 min before centrifugation to remove the cells. Glycerol concentrations were then determined in these samples using Free glycerol determination kits (Sigma-Aldrich) according to manufacturer's instructions and as previously described (61). Intracellular glycerol levels were then calculated by subtracting extracellular glycerol concentrations from total glycerol concentrations. Results shown are representative of data generated in three biological replicates, each with technical duplicates.

Cell lysis. *C. albicans* cell lysis was estimated by measuring cytosolic release. Mid-exponential-phase cells were exposed to 0 or 2 M NaCl for 10 min, cells were removed by centrifugation, and the absorbance at 260 nm was measured for the resulting supernatants. Data are expressed as the fold increase in A_{260} for stressed cells compared to the corresponding unstressed controls. Results shown represent the means (\pm SEM) of data from four biological replicates, each with technical duplicates.

Atomic force microscopy. *C. albicans* cells were grown overnight as described above, concentrated by centrifugation, washed twice in 5 ml acetate buffer (18 mM CH₃COONa, 1 mM CaCl₂, and 1 mM MnCl₂, pH 5.2), and resuspended in 3 ml of the same buffer. The cells were then immobilized on a polydimethylsiloxane (PDMS) stamp, as described before (84, 84–86), and immersed in the same acetate buffer. To gain statistical significance, about 10 to 15 cells were analyzed from three independent experiments for each strain and condition. AFM experiments were conducted on a Nanowizard III system from JPK Instruments (Berlin, Germany). We used microlever cantilever (MLCT) probes from Bruker Probes with a measured spring constant (k) ranging from 0.010 to 0.018 N/m. k was measured before each experiment by the thermal noise method (87). For elasticity measurements, force maps were recorded in force volume mode and analyzed as previously described (84, 85).

qRT-PCR. For quantitative reverse transcription-PCR (qRT-PCR) analysis, *C. albicans* cells were fixed in RNAlater according to the instructions of the manufacturer (Qiagen, Crawley, United Kingdom). Cells from 5 ml of each culture were collected and resuspended in 600 μ l QIAzol reagent (Qiagen, Crawley, United Kingdom); an equal volume of acid-washed glass beads was then added, and the cells were homogenized using a FastPrep-24 machine (MP Biomedicals, Luton, United Kingdom) (30-s bursts at the 6.0 m/s setting, with 5-min intervals on ice). RNA extractions were carried out using an RNeasy spin minikit (Sigma, United Kingdom) according to the manufacturer's instructions. The final RNA was collected in 30 μ l of diethyl pyrocarbonate (DEPC)-treated water. After repeated treatment with DNase I (Invitrogen, Paisley, United Kingdom), the isolated RNA was assessed with a NanoDrop ND-1000 spectrophotometer (Thermo Scientific, Loughborough, United Kingdom). To synthesize cDNA, samples were incubated at room temperature for 15 min using 2 μ g RNA, 2 μ l DNase I buffer (Invitrogen), 1.5 μ l DNase I, and 1.5 μ l RNaseOUT (Invitrogen) in a 20 μ l reaction mix to remove any contaminant DNA. cDNA was prepared using Superscript II (Invitrogen) per the manufacturer's protocol. Up to 40 ng of isolated RNA was used for qRT-PCR. Reactions for qRT-PCR were prepared in 10- μ l volumes containing 2 μ l of at least 10^6 diluted cDNA templates and the appropriate Universal Probes (see Table S2 in the supplemental material) per the manufacturer's instructions and run on a LightCycler 480 machine (Roche Applied Science, Burgess Hill, United Kingdom). All reactions were run in triplicate, with ACT1 used as a standard. The relative transcript abundances normalized to ACT1 were calculated based on the individually determined primer pair efficiencies with LightCycler 480 software (release 1.5.0).

Statistical analyses. Results from independent replicate experiments are expressed as means \pm SEM. All results were compared using a two-sample Student's *t* test, with a significance cutoff of 0.05. Significant differences relative to corresponding controls are denoted by asterisks in the figures.

SUPPLEMENTAL MATERIAL

Supplemental material for this article may be found at <http://mbio.asm.org/lookup/suppl/doi:10.1128/mBio.00986-15/-/DCSupplemental>.

Figure S1, PDF file, 0.2 MB.
Figure S2, PDF file, 0.1 MB.
Figure S3, PDF file, 0.3 MB.
Figure S4, PDF file, 0.1 MB.
Figure S5, PDF file, 0.1 MB.
Figure S6, PDF file, 0.1 MB.
Table S1, PDF file, 0.1 MB.
Table S2, PDF file, 0.1 MB.

ACKNOWLEDGMENTS

We thank Susan Budge for excellent technical support and our Microscopy and Histology Core Facility for superb electron microscopy. We also thank Christophe d'Enfert for sharing resources to generate the overexpression strains.

This work was supported by the European Commission (FINSysB, PITN-GA-2008-214004; STRIFE, ERC-2009-AdG-249793) and by the UK Biotechnology and Biological Research Council (BB/F00513X/1; BB/K017365/1), the UK Medical Research Council (G0400284), and the Wellcome Trust (080088, 088858/Z/09/Z 097377, 101873). The work was also supported by an ANR young scientist program (AFMYST project ANR-11-JSV5-001-01, no. SD 30024331) to E.D. E.D. is researcher at the Centre National de Recherche Scientifique (CNRS).

REFERENCES

- Saporito-Irwin SM, Birse CE, Sypher PS, Fonzi WA. 1995. PHR1, a pH-regulated gene of *Candida albicans*, is required for morphogenesis. *Mol Cell Biol* 15:601–613.
- Mouyna I, Fontaine T, Vai M, Monod M, Fonzi WA, Diaquin M, Popolo L, Hartland RP, Latgé JP. 2000. Glycosylphosphatidylinositol-anchored glucanoyltransferases play an active role in the biosynthesis of the fungal cell wall. *J Biol Chem* 275:14882–14889. <http://dx.doi.org/10.1074/jbc.275.20.14882>.
- Rolli E, Ragni E, Calderon J, Porello S, Fascio U, Popolo L. 2009. Immobilization of the glycosylphosphatidylinositol-anchored Gas1 protein into the chitin ring and septum is required for proper morphogenesis in yeast. *Mol Biol Cell* 20:4856–4870. <http://dx.doi.org/10.1091/mbc.E08-11-1155>.
- Torosantucci A, Boccanera M, Casalnuovo I, Pellegrini G, Cassone A. 1990. Differences in the antigenic expression of immunomodulatory mannoprotein constituents on yeast and mycelial forms of *Candida albicans*. *J Gen Microbiol* 136:1421–1428. <http://dx.doi.org/10.1099/00221287-136-7-1421>.
- Netea MG, Gow NA, Munro CA, Bates S, Collins C, Ferwerda G, Hobson RP, Bertram G, Hughes HB, Jansen T, Jacobs L, Buurman ET, Gijzen K, Williams DL, Torensma R, McKinnon A, MacCallum DM, Odds FC, Van der Meer JW, Brown AJ, Kullberg BJ. 2006. Immune sensing of *Candida albicans* requires cooperative recognition of mannans and glucans by lectin and Toll-like receptors. *J Clin Invest* 116:1642–1650. <http://dx.doi.org/10.1172/JCI27114>.
- Gow NA, Hube B. 2012. Importance of the *Candida albicans* cell wall during commensalism and infection. *Curr Opin Microbiol* 15:406–412. <http://dx.doi.org/10.1016/j.mib.2012.04.005>.
- Wagener J, Malireddi RK, Lenardon MD, Köberle M, Vautier S, MacCallum DM, Biedermann T, Schaller M, Netea MG, Kanneganti TD, Brown GD, Brown AJ, Gow NA. 2014. Fungal chitin dampens inflammation through IL-10 induction mediated by NOD2 and TLR9 activation. *PLoS Pathog* 10:e1004050. <http://dx.doi.org/10.1371/journal.ppat.1004050>.
- Cabib E, Roberts R, Bowers B. 1982. Synthesis of the yeast cell wall and its regulation. *Annu Rev Biochem* 51:763–793. <http://dx.doi.org/10.1146/annurev.bi.51.070182.003555>.
- Beauvais A, Latgé JP. 2001. Membrane and cell wall targets in *Aspergillus fumigatus*. *Drug Resist Updat* 4:38–49. <http://dx.doi.org/10.1054/drup.2001.0185>.
- De Groot PW, de Boer AD, Cunningham J, Dekker HL, de Jong L, Hellingwerf KJ, de Koster C, Klis FM. 2004. Proteomic analysis of *Candida albicans* cell walls reveals covalently bound carbohydrate-active enzymes and adhesins. *Eukaryot Cell* 3:955–965. <http://dx.doi.org/10.1128/EC.3.4.955-965.2004>.
- Bowman SM, Free SJ. 2006. The structure and synthesis of the fungal cell wall. *BioEssays* 28:799–808. <http://dx.doi.org/10.1002/bies.20441>.
- Munro CA. 2013. Chitin and glucan, the yin and yang of the fungal cell wall, implications for antifungal drug discovery and therapy. *Adv Appl Microbiol* 83:145–172. <http://dx.doi.org/10.1016/B978-0-12-407678-5.00004-0>.
- Shepherd MG. 1987. Cell envelope of *Candida albicans*. *Crit Rev Microbiol* 15:7–25. <http://dx.doi.org/10.3109/10408418709104445>.
- Klis FM. 1994. Review: cell wall assembly in yeast. *Yeast* 10:851–869. <http://dx.doi.org/10.1002/yea.320100702>.
- Kaptein JC, Hoyer LL, Hecht JE, Müller WH, Andel A, Verkleij AJ, Makarow M, Van Den Ende H, Klis FM. 2000. The cell wall architecture of *Candida albicans* wild-type cells and cell wall-defective mutants. *Mol Microbiol* 35:601–611. <http://dx.doi.org/10.1046/j.1365-2958.2000.01729.x>.
- Poulain D. 2015. *Candida albicans*, plasticity and pathogenesis. *Crit Rev Microbiol* 41:208–217. <http://dx.doi.org/10.3109/1040841X.2013.813904>.
- Lowman DW, Ferguson DA, Williams DL. 2003. Structural characterization of (1 \rightarrow 3)-beta-D-glucans isolated from blastospore and hyphal forms of *Candida albicans*. *Carbohydr Res* 338:1491–1496. [http://dx.doi.org/10.1016/S0008-6215\(03\)00169-1](http://dx.doi.org/10.1016/S0008-6215(03)00169-1).
- De Groot PW, Hellingwerf KJ, Klis FM. 2003. Genome-wide identification of fungal GPI proteins. *Yeast* 20:781–796. <http://dx.doi.org/10.1002/yea.1007>.
- Warit S, Zhang N, Short A, Walmsley RM, Oliver SG, Stateva LI. 2000. Glycosylation deficiency phenotypes resulting from depletion of GDP-mannose pyrophosphorylase in two yeast species. *Mol Microbiol* 36:1156–1166. <http://dx.doi.org/10.1046/j.1365-2958.2000.01944.x>.
- Bates S, MacCallum DM, Bertram G, Munro CA, Hughes HB, Buurman ET, Brown AJ, Odds FC, Gow NA. 2005. *Candida albicans* Pmr1p, a secretory pathway P-type Ca²⁺/Mn²⁺-ATPase, is required for glycosylation and virulence. *J Biol Chem* 280:23408–23415. <http://dx.doi.org/10.1074/jbc.M502162200>.
- Munro CA, Bates S, Buurman ET, Hughes HB, MacCallum DM, Bertram G, Atrih A, Ferguson MA, Bain JM, Brand A, Hamilton S, Westwater C, Thomson LM, Brown AJ, Odds FC, Gow NA. 2005. Mnt1p and Mnt2p of *Candida albicans* are partially redundant alpha-1,2-mannosyltransferases that participate in O-linked mannosylation and are required for adhesion and virulence. *J Biol Chem* 280:1051–1060. <http://dx.doi.org/10.1074/jbc.M411413200>.
- Bates S, Hughes HB, Munro CA, Thomas WP, MacCallum DM, Bertram G, Atrih A, Ferguson MA, Brown AJ, Odds FC, Gow NA. 2006. Outer chain N-glycans are required for cell wall integrity and virulence of *Candida albicans*. *J Biol Chem* 281:90–98. <http://dx.doi.org/10.1074/jbc.M510360200>.
- Klis FM, Sosinska GJ, de Groot PW, Brul S. 2009. Covalently linked cell wall proteins of *Candida albicans* and their role in fitness and virulence. *FEMS Yeast Res* 9:1013–1028. <http://dx.doi.org/10.1111/j.1567-1364.2009.00541.x>.
- Munro CA, Richard ML. 2012. The cell wall: glycoproteins, remodeling and regulation, p 197–223. In Calderone RA, Clancy CJ (ed), *Candida* and candidiasis, 2nd ed. ASM Press, Washington, DC.
- Munro CA, Gow NA. 2001. Chitin synthesis in human pathogenic fungi. *Med Mycol* 39(Suppl 1):41–53. <http://dx.doi.org/10.1080/mmy.39.1.41.53>.
- Kollár R, Reinhold BB, Petráková E, Yeh HJ, Ashwell G, Drgonová J, Kaptein JC, Klis FM, Cabib E. 1997. Architecture of the yeast cell wall. Beta(1 \rightarrow 6)-glucan interconnects mannoprotein, beta(1 \rightarrow 3)-glucan, and chitin. *J Biol Chem* 272:17762–17775. <http://dx.doi.org/10.1074/jbc.272.28.17762>.
- Munro CA, Winter K, Buchan A, Henry K, Becker JM, Brown AJ, Bulawa CE, Gow NA. 2001. Chs1 of *Candida albicans* is an essential chitin

- synthase required for synthesis of the septum and for cell integrity. *Mol Microbiol* 39:1414–1426. <http://dx.doi.org/10.1046/j.1365-2958.2001.02347.x>.
28. Ragni E, Fontaine T, Gissi C, Latgé JP, Popolo L. 2007. The Gac family of proteins of *Saccharomyces cerevisiae*: characterization and evolutionary analysis. *Yeast* 24:297–308. <http://dx.doi.org/10.1002/yea.1473>.
 29. Cabib E. 2009. Two novel techniques for determination of polysaccharide cross-links show that Crh1p and Crh2p attach chitin to both beta(1–6)- and beta(1–3)glucan in the *Saccharomyces cerevisiae* cell wall. *Eukaryot Cell* 8:1626–1636. <http://dx.doi.org/10.1128/EC.00228-09>.
 30. Fonzi WA. 1999. PHR1 and PHR2 of *Candida albicans* encode putative glycosidases required for proper cross-linking of beta-1,3- and beta-1,6-glucans. *J Bacteriol* 181:7070–7079.
 31. Alberti-Segui C, Morales AJ, Xing H, Kessler MM, Willins DA, Weinstock KG, Cottarel G, Fechtel K, Rogers B. 2004. Identification of potential cell-surface proteins in *Candida albicans* and investigation of the role of a putative cell-surface glycosidase in adhesion and virulence. *Yeast* 21:285–302. <http://dx.doi.org/10.1002/yea.1061>.
 32. Pardini G, De Groot PW, Coste AT, Karababa M, Klis FM, de Koster CG, Sanglard D. 2006. The CRH family coding for cell wall glycosylphosphatidylinositol proteins with a predicted transglycosidase domain affects cell wall organization and virulence of *Candida albicans*. *J Biol Chem* 281:40399–40411. <http://dx.doi.org/10.1074/jbc.M606361200>.
 33. Cantarel BL, Coutinho PM, Rancurel C, Bernard T, Lombard V, Henrissat B. 2009. The carbohydrate-active EnZymes database (CAZy): an expert resource for glycomics. *Nucleic Acids Res* 37:D233–D238. <http://dx.doi.org/10.1093/nar/gkn663>.
 34. Cabib E, Bowers B, Sburlati A, Silverman SJ. 1988. Fungal cell wall synthesis: the construction of a biological structure. *Microbiol Sci* 5:370–375.
 35. Caballero-Lima D, Kaneva IN, Watton SP, Sudbery PE, Craven CJ. 2013. The spatial distribution of the exocyst and actin cortical patches is sufficient to organize hyphal tip growth. *Eukaryot Cell* 12:998–1008. <http://dx.doi.org/10.1128/EC.00085-13>.
 36. Klis FM, de Groot P, Hellingwerf K. 2001. Molecular organization of the cell wall of *Candida albicans*. *Med Mycol* 39(Suppl 1):1–8.
 37. Walker LA, Munro CA, de Bruijn I, Lenardon MD, McKinnon A, Gow NA. 2008. Stimulation of chitin synthesis rescues *Candida albicans* from echinocandins. *PLoS Pathog* 4:e1000040. <http://dx.doi.org/10.1371/journal.ppat.1000040>.
 38. Pitarch A, Sánchez M, Nombela C, Gil C. 2002. Sequential fractionation and two-dimensional gel analysis unravels the complexity of the dimorphic fungus *Candida albicans* cell wall proteome. *Mol Cell Proteomics* 1:967–982. <http://dx.doi.org/10.1074/mcp.M200062-MCP200>.
 39. Sosinska GJ, de Groot PW, Teixeira de Mattos MJ, Dekker HL, de Koster CG, Hellingwerf KJ, Klis FM. 2008. Hypoxic conditions and iron restriction affect the cell-wall proteome of *Candida albicans* grown under vagina-simulative conditions. *Microbiology* 154:510–520. <http://dx.doi.org/10.1099/mic.0.2007/012617-0>.
 40. Ene IV, Cheng SC, Netea MG, Brown AJ. 2013. Growth of *Candida albicans* cells on the physiologically relevant carbon source lactate affects their recognition and phagocytosis by immune cells. *Infect Immun* 81:238–248. <http://dx.doi.org/10.1128/IAI.01092-12>.
 41. Heilmann CJ, Sorgo AG, Mohammadi S, Sosinska GJ, de Koster CG, Brul S, de Koning LJ, Klis FM. 2013. Surface stress induces a conserved cell wall stress response in the pathogenic fungus *Candida albicans*. *Eukaryot Cell* 12:254–264. <http://dx.doi.org/10.1128/EC.00278-12>.
 42. Bruneau JM, Maillat I, Tagat E, Legrand R, Supatto F, Fudali C, Caer JP, Labas V, Lecaque D, Hodgson J. 2003. Drug induced proteome changes in *Candida albicans*: comparison of the effect of beta(1,3) glucan synthase inhibitors and two triazoles, fluconazole and itraconazole. *Proteomics* 3:325–336. <http://dx.doi.org/10.1002/pmic.200390046>.
 43. Liu TT, Lee RE, Barker KS, Lee RE, Wei L, Homayouni R, Rogers PD. 2005. Genome-wide expression profiling of the response to azole, polyene, echinocandin, and pyrimidine antifungal agents in *Candida albicans*. *Antimicrob Agents Chemother* 49:2226–2236. <http://dx.doi.org/10.1128/AAC.49.6.2226-2236.2005>.
 44. Plaine A, Walker L, Da Costa G, Mora-Montes HM, McKinnon A, Gow NA, Gaillardin C, Munro CA, Richard ML. 2008. Functional analysis of *Candida albicans* GPI-anchored proteins: roles in cell wall integrity and caspofungin sensitivity. *Fungal Genet Biol* 45:1404–1414. <http://dx.doi.org/10.1016/j.fgb.2008.08.003>.
 45. Hohmann S. 2002. Osmotic stress signaling and osmoadaptation in yeasts. *Microbiol Mol Biol Rev* 66:300–372. <http://dx.doi.org/10.1128/MMBR.66.2.300-372.2002>.
 46. Klipp E, Nordlander B, Krüger R, Gennemark P, Hohmann S. 2005. Integrative model of the response of yeast to osmotic shock. *Nat Biotechnol* 23:975–982. <http://dx.doi.org/10.1038/nbt1114>.
 47. Morris GJ, Winters L, Coulson GE, Clarke KJ. 1986. Effect of osmotic stress on the ultrastructure and viability of the yeast *Saccharomyces cerevisiae*. *J Gen Microbiol* 132:2023–2034. <http://dx.doi.org/10.1099/00221287-132-7-2023>.
 48. Slaninová I, Sesták S, Svoboda A, Farkas V. 2000. Cell wall and cytoskeleton reorganization as the response to hyperosmotic shock in *Saccharomyces cerevisiae*. *Arch Microbiol* 173:245–252. <http://dx.doi.org/10.1007/s002030000136>.
 49. Schaber J, Adrover MA, Eriksson E, Pelet S, Petelenz-Kurdiel E, Klein D, Posas F, Goksör M, Peter M, Hohmann S, Klipp E. 2010. Biophysical properties of *Saccharomyces cerevisiae* and their relationship with HOG pathway activation. *Eur Biophys J* 39:1547–1556. <http://dx.doi.org/10.1007/s00249-010-0612-0>.
 50. San Jose C, Monge R, Perez-Diaz R, Pla J, Nombela C. 1996. The mitogen-activated protein kinase homolog HOG1 gene controls glycerol accumulation in the pathogenic fungus *Candida albicans*. *J Bacteriol* 178:5850–5852.
 51. Smith DA, Nicholls S, Morgan BA, Brown AJ, Quinn J. 2004. A conserved stress-activated protein kinase regulates a core stress response in the human pathogen *Candida albicans*. *Mol Biol Cell* 15:4179–4190. <http://dx.doi.org/10.1091/mbc.E04-03-0181>.
 52. Kayingo G, Wong B. 2005. The MAP kinase Hog1p differentially regulates stress-induced production and accumulation of glycerol and D-arabitol in *Candida albicans*. *Microbiology* 151:2987–2999. <http://dx.doi.org/10.1099/mic.0.28040-0>.
 53. Navarro-García F, Eisman B, Fiuza SM, Nombela C, Pla J. 2005. The MAP kinase Mkc1p is activated under different stress conditions in *Candida albicans*. *Microbiology* 151:2737–2749. <http://dx.doi.org/10.1099/mic.0.28038-0>.
 54. Macia J, Regot S, Peeters T, Conde N, Solé R, Posas F. 2009. Dynamic signaling in the Hog1 MAPK pathway relies on high basal signal transduction. *Sci Signal* 2:ra13. <http://dx.doi.org/10.1126/scisignal.2000056>.
 55. Navarro-García F, Alonso-Monge R, Rico H, Pla J, Sentandreu R, Nombela C. 1998. A role for the MAP kinase gene MKC1 in cell wall construction and morphological transitions in *Candida albicans*. *Microbiology* 144:411–424. <http://dx.doi.org/10.1099/00221287-144-2-411>.
 56. Monge RA, Román E, Nombela C, Pla J. 2006. The MAP kinase signal transduction network in *Candida albicans*. *Microbiology* 152:905–912. <http://dx.doi.org/10.1099/mic.0.28616-0>.
 57. Román E, Cottier F, Ernst JF, Pla J. 2009. Msb2 signaling mucin controls activation of Cek1 mitogen-activated protein kinase in *Candida albicans*. *Eukaryot Cell* 8:1235–1249. <http://dx.doi.org/10.1128/EC.00081-09>.
 58. Ene IV, Adya AK, Wehmeier S, Brand AC, MacCallum DM, Gow NA, Brown AJ. 2012. Host carbon sources modulate cell wall architecture, drug resistance and virulence in a fungal pathogen. *Cell Microbiol* 14:1319–1335. <http://dx.doi.org/10.1111/j.1462-5822.2012.01813.x>.
 59. Arana DM, Nombela C, Alonso-Monge R, Pla J. 2005. The Pbs2 MAP kinase kinase is essential for the oxidative-stress response in the fungal pathogen *Candida albicans*. *Microbiology* 151:1033–1049. <http://dx.doi.org/10.1099/mic.0.27723-0>.
 60. Román E, Nombela C, Pla J. 2005. The Sho1 adaptor protein links oxidative stress to morphogenesis and cell wall biosynthesis in the fungal pathogen *Candida albicans*. *Mol Cell Biol* 25:10611–10627. <http://dx.doi.org/10.1128/MCB.25.23.10611-10627.2005>.
 61. You T, Ingram P, Jacobsen MD, Cook E, McDonagh A, Thorne T, Lenardon MD, de Moura AP, Romano MC, Thiel M, Stumpf M, Gow NA, Haynes K, Grebogi C, Stark J, Brown AJ. 2012. A systems biology analysis of long and short-term memories of osmotic stress adaptation in fungi. *BMC Res Notes* 5:258. <http://dx.doi.org/10.1186/1756-0500-5-258>.
 62. Navarro-García F, Sánchez M, Pla J, Nombela C. 1995. Functional characterization of the MKC1 gene of *Candida albicans*, which encodes a mitogen-activated protein kinase homolog related to cell integrity. *Mol Cell Biol* 15:2197–2206.
 63. Douglas CM, D'Ippolito JA, Shei GJ, Meinz M, Onishi J, Marrinan JA, Li W, Abruzzo GK, Flattery A, Bartizal K, Mitchell A, Kurtz MB. 1997. Identification of the FKS1 gene of *Candida albicans* as the essential target of 1,3-beta-D-glucan synthase inhibitors. *Antimicrob Agents Chemother* 41:2471–2479.

64. Martínez AI, Castillo L, Garcerá A, Elorza MV, Valentín E, Sentandreu R. 2004. Role of Pir1 in the construction of the *Candida albicans* cell wall. *Microbiology* 150:3151–3161. <http://dx.doi.org/10.1099/mic.0.27220-0>.
65. Garcerá A, Castillo L, Martínez AI, Elorza MV, Valentín E, Sentandreu R. 2005. Anchorage of *Candida albicans* Ssr1 to the cell wall, and transcript profiling of the null mutant. *Res Microbiol* 156:911–920. <http://dx.doi.org/10.1016/j.resmic.2005.05.002>.
66. Sanglard D, Ischer F, Marchetti O, Entenza J, Bille J. 2003. Calcineurin A of *Candida albicans*: involvement in antifungal tolerance, cell morphogenesis and virulence. *Mol Microbiol* 48:959–976. <http://dx.doi.org/10.1046/j.1365-2958.2003.03495.x>.
67. Onyewu C, Wormley FL, Jr, Perfect JR, Heitman J. 2004. The calcineurin target, Crz1, functions in azole tolerance but is not required for virulence of *Candida albicans*. *Infect Immun* 72:7330–7333. <http://dx.doi.org/10.1128/IAI.72.12.7330-7333.2004>.
68. Karababa M, Valentino E, Pardini G, Coste AT, Bille J, Sanglard D. 2006. CRZ1, a target of the calcineurin pathway in *Candida albicans*. *Mol Microbiol* 59:1429–1451. <http://dx.doi.org/10.1111/j.1365-2958.2005.05037.x>.
69. Farkas V. 1979. Biosynthesis of cell walls of fungi. *Microbiol Rev* 43:117–144.
70. Wessels JGH. 1990. Role of cell wall architecture in fungal tip growth generation, p 1–29. In Heath IB (ed), *Tip growth in plant and fungal cells*. Academic Press, San Diego, CA.
71. Sosinska GJ, de Koning LJ, de Groot PW, Manders EM, Dekker HL, Hellingwerf KJ, de Koster CG, Klis FM. 2011. Mass spectrometric quantification of the adaptations in the wall proteome of *Candida albicans* in response to ambient pH. *Microbiology* 157:136–146. <http://dx.doi.org/10.1099/mic.0.044206-0>.
72. Ene IV, Heilmann CJ, Sorgo AG, Walker LA, de Koster CG, Munro CA, Klis FM, Brown AJ. 2012. Carbon source-induced reprogramming of the cell wall proteome and secretome modulates the adherence and drug resistance of the fungal pathogen *Candida albicans*. *Proteomics* 12:3164–3179. <http://dx.doi.org/10.1002/pmic.201200228>.
73. Kim YT, Kim EH, Cheong C, Williams DL, Kim CW, Lim ST. 2000. Structural characterization of beta-D-(1 → 3, 1 → 6)-linked glucans using NMR spectroscopy. *Carbohydr Res* 328:331–341. [http://dx.doi.org/10.1016/S0008-6215\(00\)00105-1](http://dx.doi.org/10.1016/S0008-6215(00)00105-1).
74. Sugawara T, Takahashi S, Osumi M, Ohno N. 2004. Refinement of the structures of cell-wall glucans of *Schizosaccharomyces pombe* by chemical modification and NMR spectroscopy. *Carbohydr Res* 339:2255–2265. <http://dx.doi.org/10.1016/j.carres.2004.05.033>.
75. Alonso-Monge R, Navarro-García F, Molero G, Diez-Orejas R, Gustin M, Pla J, Sánchez M, Nombela C. 1999. Role of the mitogen-activated protein kinase Hog1p in morphogenesis and virulence of *Candida albicans*. *J Bacteriol* 181:3058–3068.
76. Cheetham J, Smith DA, da Silva Dantas A, Doris KS, Patterson MJ, Bruce CR, Quinn J. 2007. A single MAPKKK regulates the Hog1 MAPK pathway in the pathogenic fungus *Candida albicans*. *Mol Biol Cell* 18:4603–4614. <http://dx.doi.org/10.1091/mbc.E07-06-0581>.
77. Su C, Lu Y, Liu H. 2013. Reduced TOR signaling sustains hyphal development in *Candida albicans* by lowering Hog1 basal activity. *Mol Biol Cell* 24:385–397. <http://dx.doi.org/10.1091/mbc.E12-06-0477>.
78. Odds FC, Webster CE, Mayuranathan P, Simmons PD. 1988. *Candida* and candidosis. Bailliere Tindall, London, United Kingdom.
79. Calderone RA, Clancy CJ (eds). 2011. *Candida* and candidiasis. ASM Press, Washington, DC.
80. Ghannoum MA, Spellberg B, Saporito-Irwin SM, Fonzi WA. 1995. Reduced virulence of *Candida albicans* PHR1 mutants. *Infect Immun* 63:4528–4530.
81. De Bernardis F, Mühlischlegel FA, Cassone A, Fonzi WA. 1998. The pH of the host niche controls gene expression in and virulence of *Candida albicans*. *Infect Immun* 66:3317–3325.
82. Chauvel M, Nesseir A, Cabral V, Znaidi S, Goyard S, Bachellier-Bassi S, Firon A, Legrand M, Diogo D, Naulleau C, Rossignol T, d'Enfert C. 2012. A versatile overexpression strategy in the pathogenic yeast *Candida albicans*: identification of regulators of morphogenesis and fitness. *PLoS One* 7:e45912. <http://dx.doi.org/10.1371/journal.pone.0045912>.
83. Murad AM, Lee PR, Broadbent ID, Barelle CJ, Brown AJ. 2000. CIp10, an efficient and convenient integrating vector for *Candida albicans*. *Yeast* 16:325–327.
84. Dague E, Jauvert E, Laplatine L, Viallet B, Thibault C, Ressler L. 2011. Assembly of live micro-organisms on microstructured PDMS stamps by convective/capillary deposition for AFM bio-experiments. *Nanotechnology* 22:395102. <http://dx.doi.org/10.1088/0957-4484/22/39/395102>.
85. Dague E, Bitar R, Ranchon H, Durand F, Yken HM, François JM. 2010. An atomic force microscopy analysis of yeast mutants defective in cell wall architecture. *Yeast* 27:673–684. <http://dx.doi.org/10.1002/yea.1801>.
86. Formosa C, Pillet F, Schiavone M, Duval RE, Ressler L, Dague E. 2015. Generation of living cell arrays for atomic force microscopy studies. *Nat Protoc* 10:199–204. <http://dx.doi.org/10.1038/nprot.2015.004>.
87. Hutter JL, Bechhoefer J. 1993. Calibration of atomic-force microscope tips. *Rev Sci Instrum* 64:1868. <http://dx.doi.org/10.1063/1.1143970>.
88. Fonzi WA, Irwin MY. 1993. Isogenic strain construction and gene mapping in *Candida albicans*. *Genetics* 134:717–728.
89. Negrodo A, Monteoliva L, Gil C, Pla J, Nombela C. 1997. Cloning, analysis and one-step disruption of the ARG5,6 gene of *Candida albicans*. *Microbiology* 143:297–302. <http://dx.doi.org/10.1099/00221287-143-2-297>.
90. Wilson RB, Davis D, Mitchell AP. 1999. Rapid hypothesis testing with *Candida albicans* through gene disruption with short homology regions. *J Bacteriol* 181:1868–1874.
91. Davis D, Edwards JE, Jr, Mitchell AP, Ibrahim AS. 2000. *Candida albicans* RIM101 pH response pathway is required for host-pathogen interactions. *Infect Immun* 68:5953–5959. <http://dx.doi.org/10.1128/IAI.68.10.5953-5959.2000>.
92. Noble SM, Johnson AD. 2005. Strains and strategies for large-scale gene deletion studies of the diploid human fungal pathogen *Candida albicans*. *Eukaryot Cell* 4:298–309. <http://dx.doi.org/10.1128/EC.4.2.298-309.2005>.
93. Dennison PM, Ramsdale M, Manson CL, Brown AJ. 2005. Gene disruption in *Candida albicans* using a synthetic, codon-optimised Cre-loxP system. *Fungal Genet Biol* 42:737–748. <http://dx.doi.org/10.1016/j.fgb.2005.05.006>.
94. Csank C, Schröppel K, Leberer E, Harcus D, Mohamed O, Meloche S, Thomas DY, Whiteway M. 1998. Roles of the *Candida albicans* mitogen-activated protein kinase homolog, Cek1p, in hyphal development and systemic candidiasis. *Infect Immun* 66:2713–2721.
95. Nagahashi S, Mio T, Ono N, Yamada-Okabe T, Arisawa M, Bussey H, Yamada-Okabe H. 1998. Isolation of CaSLN1 and CaNIK1, the genes for osmosensing histidine kinase homologues, from the pathogenic fungus *Candida albicans*. *Microbiology* 144:425–432. <http://dx.doi.org/10.1099/00221287-144-2-425>.
96. Nicholls S, Straffon M, Enjalbert B, Nantel A, Macaskill S, Whiteway M, Brown AJ. 2004. Msn2- and Msn4-like transcription factors play no obvious roles in the stress responses of the fungal pathogen *Candida albicans*. *Eukaryot Cell* 3:1111–1123. <http://dx.doi.org/10.1128/EC.3.5.1111-1123.2004>.
97. Zaragoza O, Blazquez MA, Gancedo C. 1998. Disruption of the *Candida albicans* TPS1 gene encoding trehalose-6-phosphate synthase impairs formation of hyphae and decreases infectivity. *J Bacteriol* 180:3809–3815.
98. Mühlischlegel FA, Fonzi WA. 1997. PHR2 of *Candida albicans* encodes a functional homolog of the pH-regulated gene PHR1 with an inverted pattern of pH-dependent expression. *Mol Cell Biol* 17:5960–5967.
99. Homann OR, Dea J, Noble SM, Johnson AD. 2009. A phenotypic profile of the *Candida albicans* regulatory network. *PLoS Genet* 5:e1000783. <http://dx.doi.org/10.1371/journal.pgen.1000783>.